

Unforeseen plant phenotypic diversity in a dry and grazed world

<https://doi.org/10.1038/s41586-024-07731-3>

Received: 22 June 2023

Accepted: 18 June 2024

Published online: 7 August 2024

 Check for updates

Earth harbours an extraordinary plant phenotypic diversity¹ that is at risk from ongoing global changes^{2,3}. However, it remains unknown how increasing aridity and livestock grazing pressure—two major drivers of global change^{4–6}—shape the trait covariation that underlies plant phenotypic diversity^{1,7}. Here we assessed how covariation among 20 chemical and morphological traits responds to aridity and grazing pressure within global drylands. Our analysis involved 133,769 trait measurements spanning 1,347 observations of 301 perennial plant species surveyed across 326 plots from 6 continents. Crossing an aridity threshold of approximately 0.7 (close to the transition between semi-arid and arid zones) led to an unexpected 88% increase in trait diversity. This threshold appeared in the presence of grazers, and moved toward lower aridity levels with increasing grazing pressure. Moreover, 57% of observed trait diversity occurred only in the most arid and grazed drylands, highlighting the phenotypic uniqueness of these extreme environments. Our work indicates that drylands act as a global reservoir of plant phenotypic diversity and challenge the pervasive view that harsh environmental conditions reduce plant trait diversity^{8–10}. They also highlight that many alternative strategies may enable plants to cope with increases in environmental stress induced by climate change and land-use intensification.

The recent development of global trait databases¹¹ has been instrumental for characterizing the phenotypic diversity (hereafter referred to as trait diversity) of the entire plant kingdom^{1,7,12}. This characterization is fundamental for anticipating the effects of global change on biodiversity and the functioning of the biosphere^{2,13}. Yet, our understanding of plant trait diversity has been biased towards mesic biomes^{14,15} (for example, temperate regions). Although the geographical coverage of trait observations is currently increasing¹¹, many regions of the globe remain poorly explored^{14,15}. In particular, drylands remain largely underrepresented in global trait databases¹⁵ (Supplementary Table 1) despite the fact that they cover around 45% of the planet's terrestrial area¹⁶, are present over all latitudes and continents¹⁷, and are projected to expand owing to climate change and associated increases in aridity¹⁸ (defined as $1 - \text{aridity index}^5$, where aridity index = mean annual precipitation/potential evapotranspiration)¹⁹. Drylands are highly vulnerable to multiple global change drivers^{4–6} including changes in aridity and pressure from livestock grazing, the major land use across drylands⁶. For instance, crossing an aridity threshold of 0.7 or increasing grazing pressure can lead to abrupt and systemic changes in multiple ecosystem attributes^{5,6}, including drastic decreases in plant species richness and cover that may lead to land degradation and desertification²⁰. However, it remains almost completely unknown how increasing aridity and grazing pressure might jointly shape trait diversity of drylands at a global scale. This knowledge is needed to make reliable predictions of the future of biodiversity^{2,13} and the functioning of dryland ecosystems^{17,21} under global change.

One may expect that crossing aridity thresholds and increasing grazing pressure should reduce trait diversity in drylands²² by selecting only those species able to tolerate extreme temperatures, low

soil nutrient contents and water availability, and high stocking rates (see the pervasive 'environmental filtering' concept^{8–10} and associated hypotheses in Supplementary Text 1 and Supplementary Fig. 1). However, drylands can exhibit a remarkable diversity of plant forms and functions^{22,23} (the 'functional paradox of drylands'¹⁷), which seemingly contradicts the environmental filtering concept. This paradox may arise because distinct trait syndromes can perform equally in response to a specific environmental constraint^{24,25}, thus allowing alternative plant strategies to persist in harsh environments (Supplementary Text 1). Given the importance of trait diversity in the provisioning of essential ecosystem services²⁶ to the more than 2 billion people inhabiting dryland areas²⁰, understanding this discrepancy is a crucial research need.

Plant traits covary predictably among species because of evolutionary and ecological constraints limiting the number of viable trait combinations^{1,7,12} that ultimately determine the extent of plant trait diversity¹. Global initiatives that aim to characterize the fundamental dimensions of trait covariation have focused mainly on plant morphological diversity^{1,7,12} and leaf carbon economy²⁷, but have largely neglected the diversity of chemical elements that sustain plant survival and growth^{28,29}. The elemental concentration in plant leaves (the plant elementome) has major implications for plant development³⁰, animal and human health^{31,32}, and global biogeochemical cycles²⁸. Furthermore, the plant elementome has a pivotal role in determining plant responses to water scarcity^{33–35} and herbivory^{36,37} (Supplementary Table 2). However, we do not know how the plant elementome is distributed across plant species and how it contributes to trait diversity patterns across global drylands. Accounting for the plant elementome may thus reveal new functional dimensions with the potential to change

A list of authors and their affiliations appears at the end of the paper.

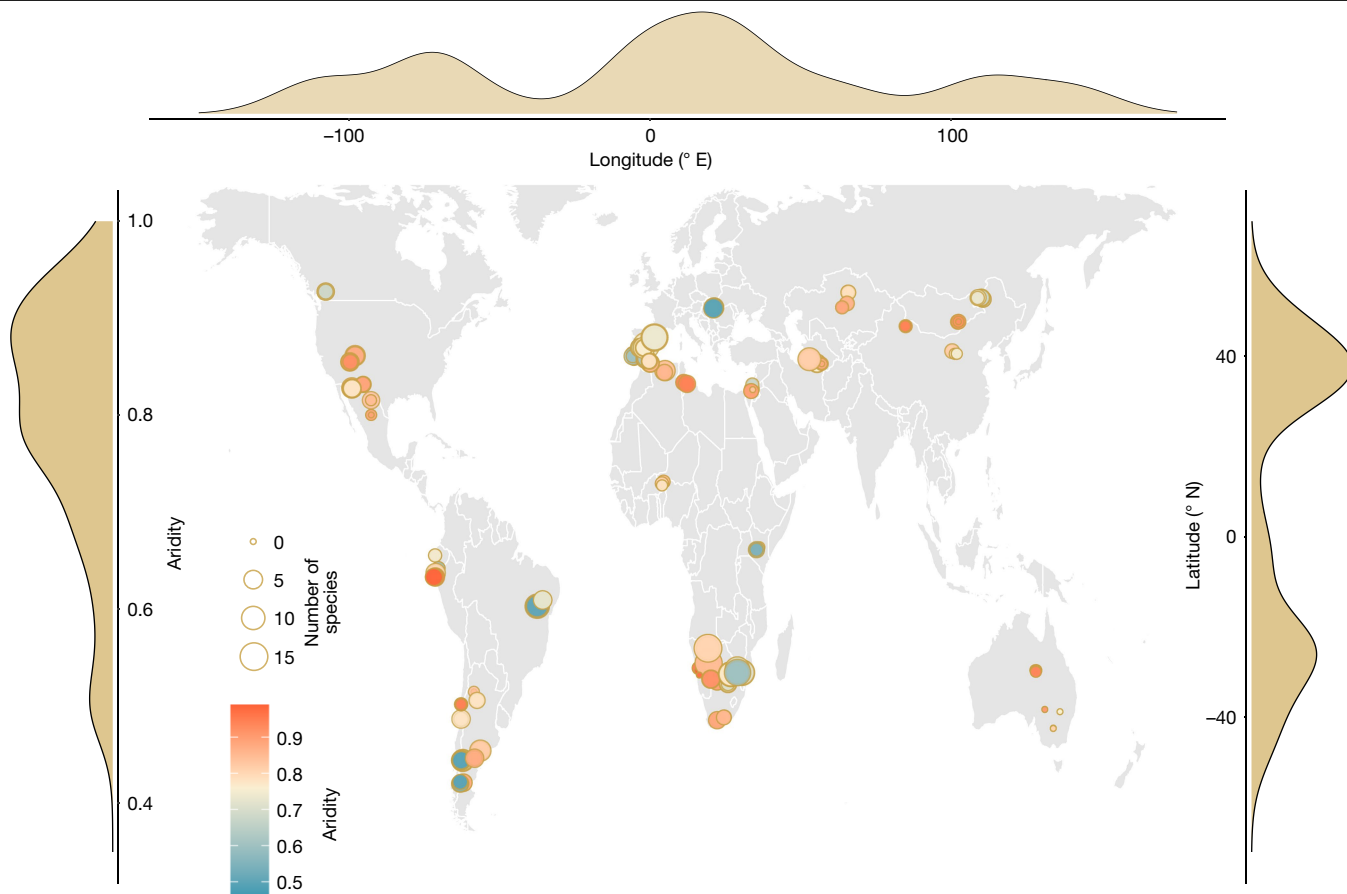


Fig. 1 | A survey of plant trait diversity across global dryland rangelands.

The data included 1,347 observations of 301 perennial plant species, which provided a complete set of measurements for the 20 traits (see Supplementary Table 3 for details). The colour of the dots represents the aridity level of each of the 98 dryland sites where plant traits have been measured. Each site included three to four plots locally distributed along a grazing gradient (326 plots were surveyed in total; Methods). The size of the dots indicates the number of

species sampled in each plot (mean number per plot = 4.6 species; minimum number per plot = 1 species; maximum number per plot = 18 species). The selected sites were globally distributed across all latitudes and continents (except Antarctica), and are representative of the wide variation in climates, soil properties and vegetation types found across global drylands^{6,17}. The distribution of the 98 sites along the aridity gradient, the longitude and the latitude are shown along the left, top and right edges of the figure, respectively.

our understanding of plant strategies in drylands and their responses to ongoing global changes.

We conducted a standardized field survey to investigate the impacts of aridity and grazing pressure on the chemical and morphological trait diversity of perennial plants across drylands worldwide (Fig. 1). We selected 98 sites from 25 countries that represent the aridity gradient over which dryland rangelands can be found globally⁶. Each site included three to four 45 m × 45 m plots spanning local gradients of grazing pressure (from ungrazed or low grazing pressure to high grazing pressure), with a total of 326 plots surveyed. In each plot, we measured a total of 20 continuous traits related to: (1) the concentration of 14 chemical elements in plant leaves (C, N, P, K, Mg, Ca, S, Zn, Na, Cu, Mn, Fe, Ba and Al); (2) the leaf and whole plant size (lateral spread, maximum plant height, leaf length and leaf area); and (3) the leaf carbon economy (specific leaf area (SLA) and leaf dry matter content (LDMC)). Our study included 1,347 observations of 301 dryland plant species sampled across 326 plots from all latitudes and continents (Fig. 1) for which the complete set of these 20 traits was measured (total number of traits measurements = 133,769; see Supplementary Table 3 for a full description of the data and Supplementary Figs. 2–4 for the frequency distribution of these traits). These data constitute a unique source of functional information to explore how aridity and grazing shape the covariations and trade-offs observed among multiple morphological and chemical plant traits across global drylands.

Trait diversity explodes in arid rangelands

We used a sliding-windows analysis (Methods) to evaluate changes in dryland trait diversity in response to increases in aridity and grazing pressure. To do so, we ordered the 326 plots surveyed according to their aridity. We then defined aridity windows that represent 19% of the global aridity gradient considered, and selected all plant species from all plots within this aridity range ($n = 307$ observations in each window). For each aridity window, we quantified the n -dimensional trait space using the plant elementome, and morphological and carbon economy-related traits (that is, trait hypervolume³⁸; see Methods and Extended Data Fig. 1, Supplementary Figs. 5–8, and Supplementary Table 4 for a description of the dryland trait space evaluated). The size of the hypervolume provides a measure of the trait diversity³⁸ considered within each aridity window.

Increases in aridity were associated with an unforeseen increase in plant trait diversity (Fig. 2a, dashed line, and Supplementary Table 5). We found a significant threshold response in the trait hypervolume occurring at an aridity value of approximately 0.7 (Fig. 2). Aridity values that exceeded this threshold were associated with an 88.1% increase in the size of the trait hypervolume in the driest rangelands surveyed (Fig. 2b and Supplementary Fig. 9). The trait hypervolume observed at high aridity levels largely encompassed and surpassed the morphological and chemical trait diversity observed under low aridity conditions: 80.1% of the low-aridity hypervolume was included within the

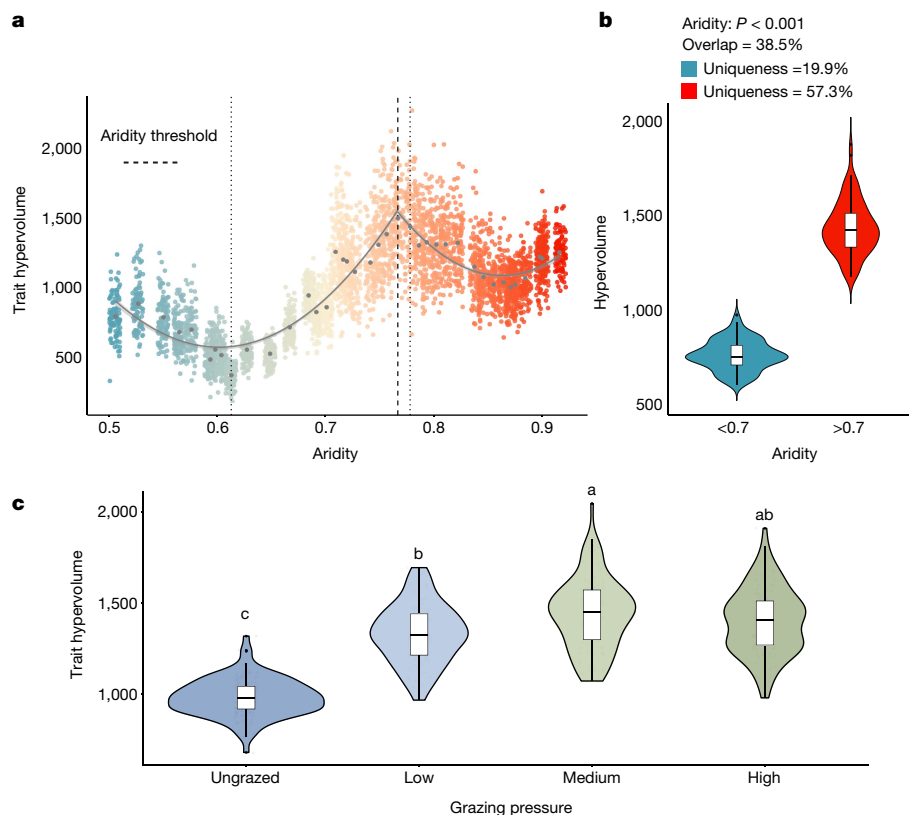


Fig. 2 | Global increase in dryland plant trait diversity driven by aridity and grazing.

a, The effect of aridity on the size of the trait hypervolume. We found a significant, non-linear increase in the hypervolume size once an aridity threshold of around 0.7 was crossed. Vertical dashed and dotted lines represent the mean location of the threshold and 95% confidence interval, respectively (Supplementary Table 5). Coloured dots represent bootstrapped values for trait hypervolume. The error band shows the 95% confidence interval. **b**, Bootstrapped values for the hypervolume size below and above the aridity threshold (low aridity, $n = 189$; high aridity, $n = 696$). After crossing the aridity threshold of approximately 0.7, the hypervolume increased by 88.1%, because it included most of the trait variability observed under low aridity conditions (only 19.9% of uniqueness) as well as 57.3% of trait diversity that

occurs only in the most arid conditions. **c**, Bootstrapped values for trait hypervolume for each grazing pressure level (high grazing, $n = 382$; medium grazing, $n = 410$; low grazing, $n = 389$; ungrazed $n = 166$). Bootstrapped values were generated using a random sampling of $n = 100$ observations for 100 times in each aridity and grazing level. In box plots, the centre line is the median, lower and upper hinges correspond to the first and third quartiles, and whiskers show the 95% confidence intervals. In **b, c**, we tested whether different aridity and grazing pressure levels showed significant differences using a generalized least squares model ($P < 0.001$ for aridity in **b** and for grazing in **c**). In **c**, letters show results of a post hoc test based on bootstrapped pairwise comparisons between grazing pressure levels; different letters indicate significant differences among grazing pressure levels.

high-aridity hypervolume and 57.3% of the global dryland trait diversity was observed only under aridity values higher than approximately 0.7 (Fig. 2b). We also observed an increase of the size of the trait hypervolume with increasing grazing pressure (Fig. 2c). Aridity and grazing thus have a similar effect on trait diversity by promoting a wide spectrum of plant strategies to cope with water shortage^{17,23,25} and herbivory^{39,40} through a variety of avoidance and tolerance strategies. Our results support theoretical predictions²⁴ and empirical observations from drylands^{17,22,23} and other extreme environments (for example, alpine ecosystems⁴¹), which suggest that there are many ways for species to cope with climatic extremes and grazing pressure. The most arid dryland rangelands thus harbour a unique trait diversity, highlighting their importance as a global reservoir of plant form and function and reinforcing the biological and evolutionary importance of dryland ecosystems.

The elementome responds to global change

The sharp increase in trait diversity observed with increases in aridity and grazing pressure resulted mainly from a decrease in trait covariation at aridity values higher than around 0.7 (Fig. 3). Specifically, both aridity (Extended Data Fig. 2 and Supplementary Table 4) and the presence of grazers (Extended Data Fig. 3 and Supplementary

Table 6) increased the number of trait dimensions within the dryland plant trait spectrum, resulting in the presence of extreme phenotypes exhibiting unique trait syndromes in the driest rangelands surveyed. For instance, all macronutrients correlated along a unique principal component axis below the -0.7 aridity threshold (principal component 1 (PC1) in Extended Data Fig. 2a, b). After exceeding the -0.7 aridity threshold, primary and secondary macronutrients—namely N-P-K and Mg-Ca-S—became independent and segregated along two different axes (Extended Data Fig. 2c–e), highlighting a decoupling between macronutrients in plants under high-aridity conditions.

High aridity levels also promoted functionally contrasting strategies (see Extended Data Fig. 4), such as tall species with fast growing leaves following stress-avoidance strategies^{22,25} (defined by high N-P-K and low LDMC values) and small conservative species following stress-tolerance strategies^{1,42} (defined by low N-P-K and high LDMC values; Extended Data Fig. 4b) with either low or high Mg-Ca (Extended Data Fig. 4a) and Zn-Na (Extended Data Fig. 4c) concentrations in leaves. These elemental strategies can reflect the contrasting role of chemical elements in plants, either as a way to tolerate high aridity levels^{33–35}, or as base elements for defensive compounds against herbivory^{36,37,43} (Supplementary Table 2). By identifying an abrupt change in trait variations among plant chemical elements occurring at aridity values of

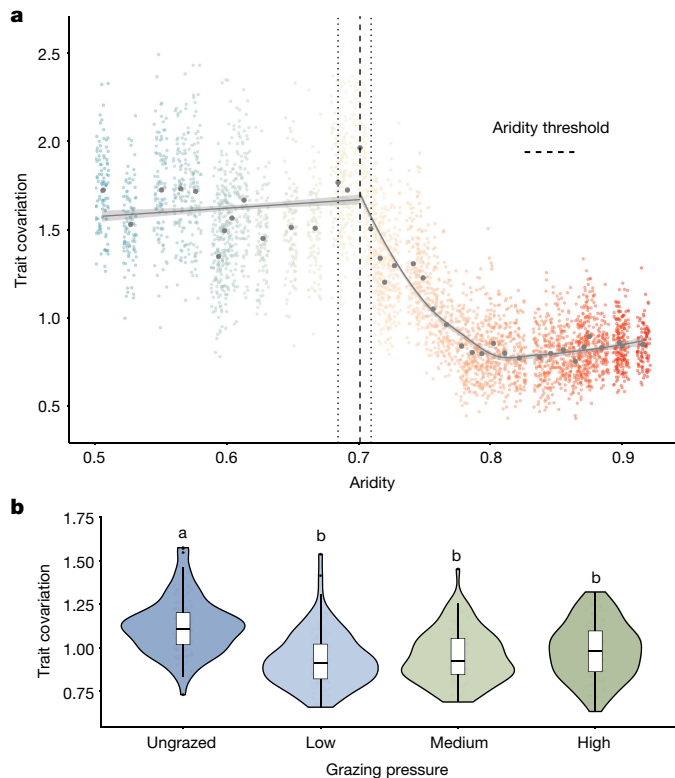


Fig. 3 | Abrupt changes in trait covariations after crossing the aridity threshold. **a**, Strength of trait covariations measured using a phenotypic integration index (Methods) decreased with aridity. We found a significant, non-linear decline at aridity values above approximately 0.7 (see Supplementary Table 5 for more detailed results). Vertical dashed and dotted lines represent the mean location of the threshold and its 95% confidence interval, respectively. Coloured dots represent bootstrapped values for trait covariation for each aridity level. The error band shows the 95% confidence interval. **b**, Bootstrapped values for trait covariation for each grazing pressure level (high grazing, $n = 382$; medium grazing, $n = 410$; low grazing, $n = 389$; ungrazed, $n = 166$). Bootstrapped values were generated using a random sampling of $n = 100$ observations for 100 times in each aridity and grazing level. In box plots, the centre line is the median, lower and upper hinges correspond to the first and third quartiles, and whiskers show the 95% confidence intervals; data beyond the confidence interval are outlying points that are plotted individually. In **b**, we tested whether different grazing pressure levels showed significant differences using a generalized least squares model ($P < 0.001$). Letters show results of a post hoc test based on bootstrapped pairwise comparisons between grazing pressure levels. Different letters indicate significant differences among grazing pressure levels.

around 0.7, our findings highlight the importance of considering the plant elementome to accurately grasp dryland biodiversity responses to ongoing climate change.

Resolving the dryland functional paradox

The abrupt increase in trait diversity with aridity observed corresponds with one of the recently identified ecosystem thresholds operating on drylands worldwide⁵, which is characterized by declines in soil fertility and plant cover after an aridity value of approximately 0.7 is crossed. The simultaneous occurrence of alterations in crucial aspects of drylands and trait diversity presents a distinctive opportunity to uncover the underlying mechanisms through which increasing aridity and grazing pressure impact on dryland ecosystems.

We first hypothesized that abrupt declines in soil fertility could explain the changes in plant trait diversity observed once the aridity threshold of approximately 0.7 is crossed. This is attributed to the fact

that variations in the chemical diversity of soils (the soil elementome) across different sites can directly affect the plant elementome^{29,44}. We tested this hypothesis by measuring the soil elemental concentration of the 326 plots surveyed (Extended Data Fig. 5 and Methods). Contrary to what is observed across plant leaves (Extended Data Fig. 1 and Supplementary Fig. 5), we found a strong covariation within the soil elementome (Extended Data Fig. 5a,b and Supplementary Fig. 10). All soil elements aligned along a unique principal component that accounts for 65.8% of the total variation observed in the soil elementome, a pattern that further increased in the most arid areas (Extended Data Fig. 5c and Supplementary Table 7). These results did not support our hypothesis. Rather, they suggested a strong decoupling between the soil and plant elementome, and therefore that plant elemental concentration reflects independent dimensions through which dryland plant species segregate across contrasting functional strategies²⁹.

Alternatively, we hypothesized that declines in plant cover may explain the observed pattern of increased trait diversity with aridity. Since the decline in plant cover can alter interactions among plants (for example, release of competitive interactions and collapse of positive interactions—including facilitation and plant–soil feedback^{5,42,45}), we expected that increasing aridity would promote the persistence of competitively weak, but well-adapted phenotypes to aridity (see Supplementary Text 2 and Supplementary Figs. 11 and 12 for a rationale for this hypothesis). To test this hypothesis, we measured in situ total plant cover across all of our sites (see Methods) and found that it was sharply reduced below around 50% after crossing the aridity threshold of approximately 0.7 (Extended Data Fig. 6). We substituted aridity with plant cover in our sliding-windows procedure, and showed that crossing a plant cover value of around 50% was associated with both an increase in the trait hypervolume and a decrease in trait covariation (Extended Data Fig. 7 and Supplementary Table 8). At cover values higher than 50%, large vegetation patches may emerge from spatial constraints only (see the ‘spanning clusters’ in percolation theory^{46–48}), forcing plant individuals to compete for space. By contrast, the decrease in plant cover below 50% may release competitive interactions as plant individuals would have space to thrive by avoiding competitive interactions^{42,45}. The match between the aridity threshold of approximately 0.7 and the 50% threshold in plant cover therefore reinforces our hypothesis that the observed pattern of increase in trait diversity with aridity may be driven by a collapse of plant–plant interactions^{5,45}. Our results challenge the pervasive environmental filtering concept^{8–10}, which posits that the abiotic environment should select for a narrow set of trait values and reduce trait diversity in the most severe environments. By contrast, they revealed that increasing plant cover and the associated biotic processes^{42,45} act as a global filter of plant biodiversity thereby reducing plant phenotypic diversity by half in the most productive compared to the most arid dryland areas.

Grazing was a main driver of decreasing plant cover (Extended Data Fig. 6a,c), and significantly modulated both the shape and location of the aridity threshold (Fig. 4 and Supplementary Table 9), indicating that climate and land use changes interact to determine phenotypic plant diversity. Specifically, the absence of grazing shifted the observed aridity threshold for trait covariation towards a higher aridity value compared with other grazing pressure levels (Fig. 4). Furthermore, removing grazing smoothed aridity effects on trait hypervolume, leading to a weak linear response of trait diversity to aridity observed in the absence of grazers (Fig. 4). Together, our results also show that by modifying plant cover, grazing pressure can modulate the response of trait diversity to increasing aridity, and thus alter the trait space of dryland plant species worldwide.

Our results shed new light on the dryland functional paradox¹⁷ by identifying a ‘plant loneliness syndrome’, in which the scattered plants across the most arid rangeland landscapes in drylands exhibit high degrees of trait uniqueness. This syndrome may result directly from the collapse of biotic interactions associated with the low

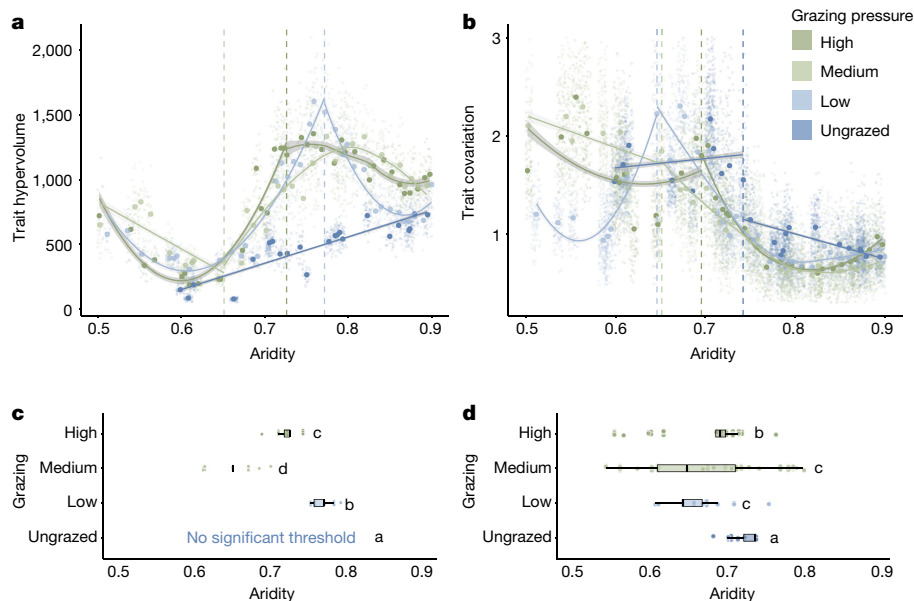


Fig. 4 | Interactions between grazing and aridity drive trait covariation and diversity across global drylands. a, b, Grazing modulates the hypervolume size (a) and trait covariation (b) in response to aridity (high grazing, $n = 382$; medium grazing, $n = 410$; low grazing, $n = 389$; ungrazed, $n = 166$). The error band shows the 95% confidence interval. Coloured dots represent bootstrapped values for trait hypervolume for each aridity level. Grazing changed both the shape of the aridity response (see Supplementary Table 9 for model selection for each grazing level) and the location of the threshold (vertical coloured dashed lines). **c, d,** Bootstrapped location of the aridity threshold at each grazing level for trait hypervolume (c) and trait covariation (d). In box plots, the centre line is the median, lower and upper hinges correspond to the first and third quartiles, and whiskers show the 95% confidence intervals; data beyond

the confidence interval are outlying points that are plotted individually. In **c, d,** we tested whether different grazing pressure levels showed significant differences using a generalized least squares model ($P < 0.001$). Letters show results of a post hoc test based on bootstrapped pairwise comparisons between grazing pressure levels. Different letters indicate significant differences among grazing pressure levels. Significant threshold responses were observed under grazing (low, medium and high grazing pressures) on trait hypervolume (**a, c**) while trait hypervolume remained constantly low as aridity increased and increased linearly when grazing was removed (ungrazed plots). For trait covariation (**b, d**), the thresholds appeared at lower aridity levels under increasing grazing pressure.

plant cover occurring in these environments^{45,48}, and from the large spatio-temporal variation in the distribution of limiting resources⁴⁹. Regardless of the mechanisms involved, the plant loneliness syndrome promotes a remarkably high plant trait diversity at the dry edge of perennial plant life. Combined with the general decline in plant taxonomic richness observed in the most arid drylands⁵, our results highlight a very low functional redundancy in the species pool of the dryland plant flora, which could compromise their resistance and resilience to further disturbances⁵⁰.

Conclusion

Here we identified an abrupt reorganization of the dryland trait space after crossing an aridity value of around 0.7. Once this threshold was reached, small increases in aridity led to an abrupt increase of trait diversity. These changes were linked to a decoupling in the plant elementome. Similarly, increases in grazing pressure substantially increased trait diversity and modulated the identified aridity threshold. Our findings illustrate how climate and land use interact to shape phenotypic plant diversity in drylands, and bring both empirical and mechanistic evidence to the dryland functional paradox¹⁷. They question the predictions of the pervasive environmental filtering concept^{8–10} that single trait optima enable species to persist in new environments. Our study also delivers insights into how vascular plants respond to biotic stressors and environmental extremes, and shed light on how the global plant functional trait space may be shaped by joint increases in aridity and grazing pressure, which are becoming more common in a drier and human-dominated world. Finally, our results can improve understanding of the provisioning of essential nutrients to livestock and human populations in drylands under ongoing global environmental change.

Online content

Any methods, additional references, Nature Portfolio reporting summaries, source data, extended data, supplementary information, acknowledgements, peer review information; details of author contributions and competing interests; and statements of data and code availability are available at <https://doi.org/10.1038/s41586-024-07731-3>.

- Díaz, S. et al. The global spectrum of plant form and function. *Nature* **529**, 167–171 (2016).
- IPBES. Summary for policymakers of the Global Assessment Report on Biodiversity and Ecosystem Services. Zenodo <https://doi.org/10.5281/zenodo.3553579> (2019).
- Carmona, C. P. et al. Erosion of global functional diversity across the tree of life. *Sci. Adv.* **7**, eabf2675 (2021).
- Shukla, P. R. et al. eds. *Climate Change and Land: An IPCC Special Report on Climate Change, Desertification, Land Degradation, Sustainable Land Management, Food Security, and Greenhouse Gas Fluxes in Terrestrial Ecosystems* (IPCC, 2019).
- Berdugo, M. et al. Global ecosystem thresholds driven by aridity. *Science* **367**, 787–790 (2020).
- Maestre, F. T. et al. Grazing and ecosystem service delivery in global drylands. *Science* **378**, 915–920 (2022).
- Joswig, J. S. et al. Climatic and soil factors explain the two-dimensional spectrum of global plant trait variation. *Nat. Ecol. Evol.* **6**, 36–50 (2022).
- Keddy, P. A. Assembly and response rules: two goals for predictive community ecology. *J. Veg. Sci.* **3**, 157–164 (1992).
- Kraft, N. J. B. et al. Community assembly, coexistence and the environmental filtering metaphor. *Funct. Ecol.* **29**, 592–599 (2015).
- Enquist, B. J. et al. in *Advances in Ecological Research*, Vol. 52 (eds Pawar, S., Woodward, G. & Dell, A. I.) 249–318 (Elsevier, 2015).
- Kattge, J. et al. TRY plant trait database—enhanced coverage and open access. *Global Change Biol.* **26**, 119–188 (2020).
- Carmona, C. P. et al. Fine-root traits in the global spectrum of plant form and function. *Nature* **597**, 683–687 (2021).
- Urban, M. C. et al. Improving the forecast for biodiversity under climate change. *Science* **353**, aad8466 (2016).
- Maitner, B. et al. A global assessment of the Raunkiaeran shortfall in plants: geographic biases in our knowledge of plant traits. *New Phytol.* **240**, 1345–1354 (2023).

15. Thomas, H. J. et al. Global plant trait relationships extend to the climatic extremes of the tundra biome. *Nat. Commun.* **11**, 1351 (2020).
16. Práville, R. Drylands extent and environmental issues. A global approach. *Earth Sci. Rev.* **161**, 259–278 (2016).
17. Maestre, F. T. et al. Biogeography of global drylands. *New Phytol.* **231**, 540–558 (2021).
18. Chai, R. et al. Human-caused long-term changes in global aridity. *npj Clim. Atmos. Sci.* **4**, 65 (2021).
19. Lian, X. et al. Multifaceted characteristics of dryland aridity changes in a warming world. *Nat. Rev. Earth Environ.* **2**, 232–250 (2021).
20. Reynolds, J. F. In *Encyclopedia of Biodiversity* (ed. Levin, S. A.) 61–78 (Elsevier, New York, 2001).
21. Van Bodegom, P. M., Douma, J. C. & Verheijen, L. M. A fully traits-based approach to modeling global vegetation distribution. *Proc. Natl Acad. Sci. USA* **111**, 13733–13738 (2014).
22. Le Bagousse-Pinguet, Y. et al. Testing the environmental filtering concept in global drylands. *J. Ecol.* **105**, 1058–1069 (2017).
23. Noy-Meir, I. Desert ecosystems: environment and producers. *Annu. Rev. Ecol. Syst.* **4**, 25–51 (1973).
24. Marks, C. O. & Lechowicz, M. J. Alternative designs and the evolution of functional diversity. *Am. Nat.* **167**, 55–66 (2006).
25. Volaire, F. A unified framework of plant adaptive strategies to drought: crossing scales and disciplines. *Global Change Biol.* **24**, 2929–2938 (2018).
26. Gross, N. et al. Functional trait diversity maximizes ecosystem multifunctionality. *Nat. Ecol. Evol.* **1**, 0132 (2017).
27. Wright, I. J. et al. The worldwide leaf economics spectrum. *Nature* **428**, 821–827 (2004).
28. Fernández-Martínez, M. From atoms to ecosystems: elementome diversity meets ecosystem functioning. *New Phytol.* **234**, 35–42 (2022).
29. Peñuelas, J. et al. The bioelements, the elementome, and the biogeochemical niche. *Ecology* **100**, e02652 (2019).
30. Baxter, I. & Dilkes, B. P. Elemental profiles reflect plant adaptations to the environment. *Science* **336**, 1661–1663 (2012).
31. White, P. J. & Brown, P. Plant nutrition for sustainable development and global health. *Ann. Bot.* **105**, 1073–1080 (2010).
32. Kaspari, M., De Beurs, K. M. & Welts, E. A. R. How and why plant ionomes vary across North American grasslands and its implications for herbivore abundance. *Ecology* **102**, e03459 (2021).
33. Lanning, M. et al. Intensified vegetation water use under acid deposition. *Sci. Adv.* **5**, eaav5168 (2019).
34. Goldack, D., Li, C., Mohan, H. & Probst, N. Tolerance to drought and salt stress in plants: unraveling the signaling networks. *Frontiers Plant Sci.* **5**, 151 (2014).
35. Morales, F., Pavlović, A., Abadía, A. & Abadía, J. In *The Leaf: A Platform for Performing Photosynthesis*, Vol. 44 (eds. Adams III, W. W. & Terashima, I.) 371–399 (Springer, 2018).
36. Mládková, P., Mládek, J., Hejduk, S., Hejzman, M. & Pakeman, R. J. Calcium plus magnesium indicates digestibility: the significance of the second major axis of plant chemical variation for ecological processes. *Ecol. Lett.* **21**, 885–895 (2018).
37. Boyd, R. Elemental defenses of plants by metals. *Nat. Educ. Knowl.* **3**, 57 (2010).
38. Blonder, B., Lamanna, C., Violle, C. & Enquist, B. J. The *n*-dimensional hypervolume. *Global Ecol. Biogeogr.* **23**, 595–609 (2014).
39. Moles, A. T. et al. Correlations between physical and chemical defences in plants: tradeoffs, syndromes, or just many different ways to skin a herbivorous cat? *New Phytol.* **198**, 252–263 (2013).
40. Briske, D. D. In *The Ecology and Management of Grazing Systems* (eds Hodgson, J. & Illius, A. W.) 37–67 (1996).
41. Körner, C. *Alpine Plant Life* (Springer, 2003); <https://doi.org/10.1007/978-3-642-18970-8>.
42. Grime, J. P. Evidence for the existence of three primary strategies in plants and its relevance to ecological and evolutionary theory. *Am. Nat.* **111**, 1169–1194 (1977).
43. He, H., Bleby, T. M., Veneklaas, E. J., Lambers, H. & Kuo, J. Precipitation of calcium, magnesium, strontium and barium in tissues of four *Acacia* species (Leguminosae: Mimosoideae). *PLoS ONE* **7**, e41563 (2012).
44. Han, W. X., Fang, J. Y., Reich, P. B., Ian Woodward, F. & Wang, Z. H. Biogeography and variability of eleven mineral elements in plant leaves across gradients of climate, soil and plant functional type in China: biogeography and variability of leaf chemistry. *Ecol. Lett.* **14**, 788–796 (2011).
45. Michalet, R., Le Bagousse-Pinguet, Y., Maalouf, J. & Lortie, C. J. Two alternatives to the stress-gradient hypothesis at the edge of life: the collapse of facilitation and the switch from facilitation to competition. *J. Veg. Sci.* **25**, 609–613 (2014).
46. Rietkerk, M. & van de Koppel, J. Alternate stable states and threshold effects in semi-arid grazing systems. *Oikos* **97**, 69–76 (1997).
47. Abades, S. R., Gaxiola, A. & Marquet, P. A. Fire, percolation thresholds and the savanna forest transition: a neutral model approach. *J. Ecol.* **102**, 1386–1393 (2014).
48. Berdugo, M. et al. Aridity preferences alter the relative importance of abiotic and biotic drivers on plant species abundance in global drylands. *J. Ecol.* **107**, 190–202 (2019).
49. Chesson, P. Mechanisms of maintenance of species diversity. *Annu. Rev. Ecol. Syst.* **31**, 343–366 (2000).
50. Biggs, C. R. et al. Does functional redundancy affect ecological stability and resilience? A review and meta-analysis. *Ecosphere* **11**, e03184 (2020).

Publisher's note Springer Nature remains neutral with regard to jurisdictional claims in published maps and institutional affiliations.

Springer Nature or its licensor (e.g. a society or other partner) holds exclusive rights to this article under a publishing agreement with the author(s) or other rightsholder(s); author self-archiving of the accepted manuscript version of this article is solely governed by the terms of such publishing agreement and applicable law.

© The Author(s), under exclusive licence to Springer Nature Limited 2024, corrected publication 2024

Nicolas Gross^{1,2,3,4}, Fernando T. Maestre^{2,3,5}, Pierre Liancourt^{3,4}, Miguel Berdugo^{5,6}, Raphaël Martin¹, Beatriz Gozalo⁷, Victoria Ochoa⁷, Manuel Delgado-Baquerizo⁸, Vincent Maire⁹, Hugo Saiz¹⁰, Santiago Soliveres^{7,11}, Enrique Valencia⁵, David J. Eldridge¹², Emilio Guirado⁷, Franck Jabot¹, Sergio Asensio⁷, Juan J. Gaitán^{13,14,15}, Miguel García-Gómez¹⁶, Paloma Martínez¹⁷, Jaime Martínez-Valderrama⁷, Betty J. Mendoza¹⁸, Eduardo Moreno-Jiménez¹⁹, David S. Pescador^{18,20}, César Plaza¹⁷, Ivan Santaolaria Pijuan⁷, Mehdi Abedi²¹, Rodrigo J. Ahumada²², Fateh Amghar²³, Antonio I. Arroyo²⁴, Khadijeh Bahalkeh²¹, Lydia Bailey²⁵, Farah Ben Salem²⁶, Niels Blaum²⁷, Bazartseren Boldgiv²⁸, Matthew A. Bowke^{25,29}, Cristina Branquinho³⁰, Liesbeth van den Brink^{4,31}, Chongfeng Bu^{32,33}, Raffaella Canessa^{4,34,35}, Andrea del P. Castillo-Monroy³⁶, Helena Castro³⁷, Patricia Castro³⁸, Roukaya Chibani³⁹, Abel Augusto Conceição⁴⁰, Anthony Darrouzet-Nardi⁴¹, Yvonne C. Davila⁴², Balázs Deák⁴³, David A. Donoso³⁶, Jorge Durán⁴⁴, Carlos Espinosa⁴⁵, Alex Fajardo^{46,47,48}, Mohammad Farzam⁴⁹, Daniela Ferrante^{50,51}, Jorgelina Franzese⁵², Lauchlan Fraser⁵³, Sofía Gonzalez⁵², Elizabeth Gusman-Montalvan⁴⁵, Rosa Mary Hernández-Hernández⁵⁴, Norbert Hölzel⁵⁵, Elisabeth Huber-Sannwald⁵⁶, Oswaldo Jadan³⁸, Florian Jeltsch²⁷, Anke Jentsch⁵⁷, Mengchen Ju^{32,33}, Kudzai F. Kaseke⁵⁸, Liana Kindermann⁵⁹, Peter le Roux⁶⁰, Anja Linstädter^{58,61}, Michelle A. Louw⁶⁰, Mancha Mabaso⁶², Gillian Maggs-Kölling⁶³, Thulani P. Makhalanyane⁶⁴, Oumarou Malam Issa⁶⁵, Antonio J. Manzaneda⁶⁶, Eugene Marais⁶³, Pierre Margerie⁶⁷, Frederic Mendes Hughes^{40,68,69}, João Vitor S. Messeder⁷⁰, Juan P. Mora⁴⁶, Gerardo Moreno⁷¹, Seth M. Munson⁷², Alice Nunes⁷⁰, Gabriel Oliva^{50,51}, Gaston R. Oñativia⁷³, Guadalupe Peter^{15,74}, Yolanda Pueyo²⁴, R. Emiliano Quiroga^{22,75}, Elizabeth Ramírez-Iglesias⁷⁶, Sasha C. Reed⁷⁷, Pedro J. Rey⁷⁸, Victor M. Reyes Gómez⁷⁹, Alexandra Rodriguez⁴⁴, Victor Rolo⁷¹, Juan G. Rubalcaba⁶², Jan C. Ruppert⁴, Osvaldo Sala⁸⁰, Ayman Salah⁸¹, Phokgedi Julius Sebeli⁸², Ilan Stav⁸³, Colton Stephens⁸⁵, Alberto L. Teixido⁵, Andrew D. Thomas⁸⁴, Heather L. Throop^{85,86}, Katja Tielbörger⁴, Samantha Travers⁸⁷, Sainbileg Undrakhbold²⁸, James Val⁸⁷, Orsolya Valkó⁴³, Frederike Velbert⁸⁵, Wanyoike Wamiti⁸⁸, Lixin Wang⁸⁹, Deli Wang⁹⁰, Glenda M. Wardle⁹¹, Peter Wolf⁸⁷, Laura Yahdjian⁷³, Reza Yari⁹², Eli Zaady⁹³, Juan Manuel Zeberio⁷⁴, Yuanling Zhang⁹⁴, Xiaobing Zhou⁹⁴ & Yoann Le Bagousse-Pinguet^{95,96,97}

¹Université Clermont Auvergne, INRAE, VetAgro Sup, Unité Mixte de Recherche Ecosystème Prairial, Clermont-Ferrand, France. ²Environmental Sciences and Engineering, Biological and Environmental Science and Engineering Division, King Abdullah University of Science and Technology, Thuwal, Kingdom of Saudi Arabia. ³Botany Department, State Museum of Natural History Stuttgart, Stuttgart, Germany. ⁴Plant Ecology Group, University of Tübingen, Tübingen, Germany. ⁵Departamento de Biodiversidad, Ecología y Evolución, Facultad de Ciencias Biológicas, Universidad Complutense de Madrid, Madrid, Spain. ⁶Department of Environmental Systems Science, ETH Zurich, Zurich, Switzerland. ⁷Instituto Multidisciplinar para el Estudio del Medio “Ramón Margalef”, Universidad de Alicante, Alicante, Spain. ⁸Laboratorio de Biodiversidad y Funcionamiento Ecosistémico. Instituto de Recursos Naturales y Agrobiología de Sevilla (IRNAS), CSIC, Sevilla, Spain. ⁹Département des Sciences de l’Environnement, Université du Québec à Trois-Rivières, Trois Rivières, Quebec, Canada. ¹⁰Departamento de Ciencias Agrarias y Medio Natural, Escuela Politécnica Superior, Instituto Universitario de Investigación en Ciencias Ambientales de Aragón (IUCA), Universidad de Zaragoza, Huesca, Spain. ¹¹Departamento de Ecología, Universidad de Alicante, Alicante, Spain. ¹²Centre for Ecosystem Science, School of Biological, Earth and Environmental Sciences, University of New South Wales, Sydney, New South Wales, Australia. ¹³Instituto Nacional de Tecnología Agropecuaria (INTA), Instituto de Suelos-CNIA, Buenos Aires, Argentina. ¹⁴Departamento de Tecnología, Universidad Nacional de Luján, Luján, Argentina. ¹⁵Consejo Nacional de Investigaciones Científicas y Técnicas de Argentina (CONICET), Buenos Aires, Argentina. ¹⁶Departamento de Ingeniería y Morfología del Terreno, Escuela Técnica Superior de Ingenieros de Caminos, Canales y Puertos, Universidad Politécnica de Madrid, Madrid, Spain. ¹⁷Instituto de Ciencias Agrarias, Consejo Superior de Investigaciones Científicas, Madrid, Spain. ¹⁸Departamento de Biología y Geología, Física y Química Inorgánica, Universidad Rey Juan Carlos, Móstoles, Spain. ¹⁹Department of Agricultural and Food Chemistry, Faculty of Sciences, Universidad Autónoma de Madrid, Madrid, Spain. ²⁰Departamento de Farmacología, Farmacognosia y Botánica, Facultad de Farmacia, Universidad Complutense de Madrid, Madrid, Spain. ²¹Department of Range Management, Faculty of Natural Resources and Marine Sciences, Tarbiat Modares University, Noor, Iran. ²²Estación Experimental Agropecuaria Catamarca, Instituto Nacional de Tecnología Agropecuaria, Catamarca, Argentina. ²³Laboratoire de Recherche: Biodiversité, Biotechnologie, Environnement et Développement Durable (BioDev), Faculté des Sciences, Université M’hamed Bougara de Boumerdès, Boumerdès, Algérie. ²⁴Instituto Pirenaico de Ecología (IPE CSIC), Zaragoza, Spain. ²⁵Center for Ecosystem Science and Society, Northern Arizona University, Flagstaff, AZ, USA. ²⁶Laboratory of Pastoral Ecosystems and Promotion of Spontaneous Plants and Associated Micro-Organisms, Institut des Régions Arides (IRA) Médenine, University of Gabes, Zrig Eddakhlania, Tunisia. ²⁷Plant Ecology and Nature Conservation, University of Potsdam, Potsdam, Germany. ²⁸Department of Biology, School of Arts and Sciences, National University of Mongolia, Ulaanbaatar, Mongolia. ²⁹School of Forestry, Northern Arizona University, Flagstaff, AZ, USA. ³⁰c3Ec — Centre for Ecology, Evolution and Environmental Changes and CHANGE — Global Change and Sustainability Institute, Faculdade de Ciências, Universidade de Lisboa, Lisboa, Portugal. ³¹ECOBIOIS, Departamento de Botánica, Universidad de Concepción, Concepción, Chile. ³²Institute of Soil and Water Conservation, Northwest A&F University, Yangling, China. ³³Institute of Soil and Water Conservation, Chinese Academy of Sciences and Ministry of Water Resources, Yangling, China. ³⁴German Centre for Integrative Biodiversity Research (iDiv) Halle-Jena-Leipzig, Leipzig, Germany. ³⁵Institut für Biologie, Martin-Luther-Universität Halle-Wittenberg, Halle, Germany. ³⁶Departamento de Biología, Escuela Politécnica Nacional, Quito, Ecuador. ³⁷Department of Life Sciences, Centre for Functional Ecology, University of

Coimbra, Coimbra, Portugal. ³⁸Facultad de Ciencias Agropecuarias, Carrera de Ingeniería Agronómica, Grupo de Agroforestería, Manejo y Conservación del Paisaje, Universidad de Cuenca, Cuenca, Ecuador. ³⁹Laboratory of Eremology and Combating Desertification, Institut des Régions Arides (IRA) Médenine, University of Gabes, Zrig Eddakhlania, Tunisia. ⁴⁰Departamento de Ciências Biológicas, Universidade Estadual de Feira de Santana, Feira de Santana, Brasil. ⁴¹Department of Biological Sciences, University of Texas at El Paso, El Paso, TX, USA. ⁴²Faculty of Science, University of Technology Sydney, Sydney, New South Wales, Australia. ⁴³Lendület Seed Ecology Research Group, Institute of Ecology and Botany, Centre for Ecological Research, Vácrátót, Hungary. ⁴⁴Misión Biolóxica de Galicia, CSIC, Pontevedra, Spain. ⁴⁵Departamento de Ciencias Biológicas y Agropecuarias, Universidad Técnica Particular de Loja, Loja, Ecuador. ⁴⁶Instituto de Investigación Interdisciplinaria (I3), Universidad de Talca, Talca, Chile. ⁴⁷Instituto de Ecología y Biodiversidad (IEB), Santiago, Chile. ⁴⁸Limits of Life (LiLi), Instituto Milenio, Valdivia, Chile. ⁴⁹Department of Range and Watershed Management, Faculty of Natural Resources and Environment, Ferdowsi University of Mashhad, Mashhad, Iran. ⁵⁰Instituto Nacional de Tecnología Agropecuaria EEA Santa Cruz, Río Gallegos, Argentina. ⁵¹Universidad Nacional de la Patagonia Austral, Río Gallegos, Argentina. ⁵²Instituto de Investigaciones en Biodiversidad y Medioambiente, Consejo Nacional de Investigaciones Científicas y Técnicas—Universidad Nacional del Comahue, Neuquen, Argentina. ⁵³Department of Natural Resource Science, Thompson Rivers University, Kamloops, British Columbia, Canada. ⁵⁴Instituto de Estudios Científicos y Tecnológicos (IDECYT); Centro de Estudios de Agroecología Tropical (CEDAT), Universidad Nacional Experimental Simón Rodríguez (UNESR), Miranda, Venezuela. ⁵⁵Institute of Landscape Ecology, University of Münster, Münster, Germany. ⁵⁶Instituto Potosino de Investigación Científica y Tecnológica, San Luis Potosí, México. ⁵⁷Department of Disturbance Ecology, Bayreuth Center of Ecology and Environmental Research BayCEER, University of Bayreuth, Bayreuth, Germany. ⁵⁸Earth Research Institute, University of California, Santa Barbara, Santa Barbara, CA, USA. ⁵⁹Biodiversity Research, Systematic Botany Group, Institute of Biochemistry and Biology, University of Potsdam, Potsdam, Germany. ⁶⁰Department of Plant and Soil Sciences, University of Pretoria, Pretoria, South Africa. ⁶¹Institute of Crop Science and Resource Conservation, University of Bonn, Bonn, Germany. ⁶²Department of Biochemistry, Genetics and Microbiology, DSI/NRF SARChI in Marine Microbiomics, University of Pretoria, Pretoria, South Africa. ⁶³Gobabeb, Namib Research Institute, Walvis Bay, Namibia. ⁶⁴Department of Microbiology, Faculty of Science, Stellenbosch University, Stellenbosch, South Africa. ⁶⁵Institut d'Écologie et des Sciences de l'Environnement de Paris (iEES-Paris), Sorbonne Université, IRD, CNRS, INRAE, Université Paris Est Creteil, Université de Paris, Centre IRD de France Nord, Bondy, France. ⁶⁶Departamento Biología Animal, Biología Vegetal y Ecología, Universidad de Jaén, Jaén, Spain. ⁶⁷Normandie Université, UNIROUEN, INRAE, ECODIV, Rouen, France. ⁶⁸Programa de Pós-Graduação em Zoologia and Conselho de Curadores das Coleções Científicas, Universidade Estadual de Santa Cruz, Ilhéus, Brazil. ⁶⁹Programa de Pós-Graduação em Bioinformática, Universidade Federal de Minas Gerais, Pampulha, Brazil. ⁷⁰Biology Department and Ecology Program, The Pennsylvania State University, University Park, PA, USA. ⁷¹Forestry School, INDEHESA, Universidad de Extremadura, Plasencia, Spain. ⁷²Southwest Biological Science Center, US Geological Survey, Flagstaff, AZ, USA. ⁷³Cátedra de Ecología, Facultad de Agronomía Instituto de Investigaciones Fisiológicas y Ecológicas Vinculadas a la Agricultura (IFEVA-CONICET), Universidad de Buenos Aires, Buenos Aires, Argentina. ⁷⁴CANPa, Universidad Nacional de Río Negro, Sede Atlántica, Río Negro, Argentina. ⁷⁵Cátedra de Manejo de Pastizales Naturales, Facultad de Ciencias Agrarias, Universidad Nacional de Catamarca, Catamarca, Argentina. ⁷⁶Universidad Estatal Amazónica (UEA), Puyo-Ecuador, Ecuador. ⁷⁷US Geological Survey, Southwest Biological Science Center, Moab, UT, USA. ⁷⁸Instituto Interuniversitario de Investigación del Sistema Tierra de Andalucía, Universidad de Jaén, Jaén, Spain. ⁷⁹Institute of Ecology, Environment and Sustainability Network, Chihuahua, Mexico. ⁸⁰Global Drylands Center, School of Life Sciences and School of Sustainability, Arizona State University, Tempe, AZ, USA. ⁸¹Al Quds University, Jerusalem, Palestine. ⁸²Mara Research Station, Limpopo Department of Agriculture and Rural Development, Polokwane, South Africa. ⁸³Dead Sea and Arava Science Center, Yotvata, Israel. ⁸⁴Department of Geography and Earth Sciences, Aberystwyth University, Aberystwyth, UK. ⁸⁵School of Earth and Space Exploration, Arizona State University, Tempe, AZ, USA. ⁸⁶School of Life Sciences, Arizona State University, Tempe, AZ, USA. ⁸⁷Department of Planning and Environment, Centre for Ecosystem Science, School of Biological, Earth and Environmental Sciences, University of New South Wales, Sydney, New South Wales, Australia. ⁸⁸Zoology Department, National Museums of Kenya, Nairobi, Kenya. ⁸⁹Department of Earth and Environmental Sciences, Indiana University Indianapolis (IU), Indianapolis, IN, USA. ⁹⁰Key Laboratory of Vegetation Ecology of the Ministry of Education, Jilin Songnen Grassland Ecosystem National Observation and Research Station, Institute of Grassland Science, Northeast Normal University, Changchun, China. ⁹¹Desert Ecology Research Group, School of Life and Environmental Sciences, The University of Sydney, Sydney, New South Wales, Australia. ⁹²Forest and Rangeland Research Department, Khorasan Razavi Agricultural and Natural Resources Research and Education Center, AREEO, Mashhad, Iran. ⁹³Gilat Research Center, Department of Natural Resources, Institute of Plant Sciences, Agricultural Research Organization, Rishon LeZion, Israel. ⁹⁴State Key Laboratory of Desert and Oasis Ecology, Key Laboratory of Ecological Safety and Sustainable Development in Arid Lands, Xinjiang Institute of Ecology and Geography, Chinese Academy of Sciences, Beijing, China. ⁹⁵Aix Marseille Univ, CNRS, Avignon Université, IRD, IMBE, Aix-en-Provence, France. ⁹⁶e-mail: nicolas.gross@inrae.fr; fernando.maestregil@kaust.edu.sa; yoann.pinguet@imbe.fr

Methods

Further details on methods are given in the Supplementary Information.

Study site selection

Our study focused on drylands, areas where rainfall is <65% of the evaporative demand⁵¹. We surveyed 98 dryland sites located in 25 countries from six continents (Algeria, Argentina, Australia, Botswana, Brazil, Canada, Chile, China, Ecuador, Hungary, Iran, Israel, Kazakhstan, Kenya, Mexico, Mongolia, Namibia, Niger, Palestine, Peru, Portugal, South Africa, Spain, Tunisia and the USA) (Fig. 1). Site selection captured most of the aridity conditions, vegetation (shrublands, grasslands, open woodlands, savannahs and steppes) and soil types that can be found in drylands worldwide (see refs. 6, 52 for more detailed explanation on site selection). At each of the 98 study sites surveyed, three to four 45 m × 45 m plots (total $n = 326$ plots) were selected along a local grazing gradient (ungrazed, low, medium and high grazing pressure), which was largely driven by livestock (but also included native herbivores⁶). Each grazing gradient was established using the distance to artificial water points and grazing exclosures when available (see ref. 6 for a detailed assessment of the validation of the local grazing gradients surveyed). In our dataset, aridity⁵¹ was defined as $1 - \text{aridity index}$, where aridity index is mean annual precipitation/potential evapotranspiration, following ref. 5. Aridity ranged between 0.48 (wettest) to 0.99 (driest) across the surveyed drylands. This aridity range corresponds to a gradient of mean annual precipitation between 891 and 29 mm yr⁻¹, and to a gradient of mean annual temperature between -1.2 and 29.2 °C. Our survey also captured most of the variation in grazing pressure that can be found across dryland rangelands worldwide⁶.

Plant trait sampling

Fieldwork was conducted between January 2016 and September 2019. Vegetation surveys were carried out after the main rainfall season at each site to ensure surveying during (or just after) the main peak biomass. This approach allowed us to standardize the sampling while accounting for differences in vegetation phenology among contrasted biogeographical regions, continents, and hemispheres. We restricted our study to perennial plants because they represent 94% of the plant species on earth⁵³ and are instrumental in maintaining the functioning of drylands^{26,54–56}.

We focused on 20 continuous traits related to the morphological and chemical diversity of plants, which were measured following the most updated standardized protocols^{57,58}. These traits included: (1) whole-plant and leaf size related traits^{1,59} (maximum plant height (H , in cm), plant lateral spread (LS, in cm²), leaf length (LL, in cm) and leaf area (LA, in cm²)); (2) leaf traits related to carbon economy and herbivory^{27,32,40,60,61} (SLA (in cm² g⁻¹) and LDMC (in g g⁻¹)); and (3) the foliar concentration of 14 chemical elements that characterize the plant elementome^{28,29,32,62} (C, N, P, K, Mg, Ca, Zn, S, Na, Cu, Fe, Al, Mn and Ba). These traits were measured in situ within each of the 326 plots. To do so, four 45 m transects oriented downslope were established within each plot, and spaced 10 m apart. We then placed 25 contiguous quadrats (1.5 m × 1.5 m) along each transect (100 quadrats per plot). Trait measurements were performed on five quadrats randomly selected in each transect (5 quadrats × 4 transects = 20 quadrats per plot). In each quadrat, we selected the most developed individual of each perennial species present. Our sampling protocol is highly suitable to account for both local trait abundances (because frequent species will have more samples than rare species^{63,64}) and between-plot intraspecific trait variability⁶⁵. See ref. 52 for a detailed description of the sampling protocol followed.

We measured plant height (the height of the selected individual from the ground to the highest leaves belonging to the vegetative part of the plant) and the lateral spread using two perpendicular measurements of plant width. On the same individual, we then sampled

mature and undamaged leaves at the top of the plant to ensure a development under full-light conditions (sampled leaf surface was always > 2 cm²). Leaves were stored in moistened plastic bags and brought to the laboratory for rehydration, before leaf area and leaf mass measurements.

We measured the leaf area of each sampled individual by taking pictures of the collected leaves flattened below a glass sheet and analysed them using ImageJ⁶⁶ (<https://imagej.nih.gov/ij/index.html>; see ref. 52 for additional details). Leaf fresh and dry mass for each sampled individual were obtained by weighing before and after oven drying at 60 °C for 48 h. Then, dry leaves were grouped by species within each plot in paper bags and were shipped to the laboratory of Rey Juan Carlos University in Móstoles (Spain) for chemical analyses. These shipments were carried out according to national and international regulations; exporting permits were obtained for each country (when required) and importing permits to Spain were obtained for every shipment by the Spanish Ministry of Agriculture, Fisheries and Food.

Once in the laboratory, oven-dried leaves were ground in a homogenizer (Precellys 24; Bertin Technologies) and analysed for total nitrogen and total carbon on a EuroEA3000 elemental analyser (EuroVector). Total chemical elements in leaves (P, K, Mg, Ca, Cu, Zn, S, Na, Fe, Al, Mn and Ba) were analysed by inductively coupled plasma optical emission spectrometry with a Perkin Elmer Optima 4300 DV (Perkin Elmer) after open-vessel nitric-perchloric acid wet digestion. At the end of this procedure, we obtained the foliar concentration of the 14 elements for each species sampled in each plot.

Plant cover and soil properties measurements

We quantified vegetation cover in each plot using the line-point intercept method⁵². We recorded points located every 20 cm along each of the four transects for a total of 225 points per transect (900 points per plot; see ref. 54 for additional details on this survey). Vegetation cover was calculated as the proportion of points where perennial plants were recorded.

We also quantified the elemental concentrations of the soil beneath plant canopies in each of the 326 plots surveyed in the peak of the dry season to ensure that the data obtained across sites were as standardized and comparable as possible⁶. At each plot, five 50 cm × 50 cm quadrats were randomly placed under the canopy of the dominant (in terms of percentage cover) perennial plant species. A composite topsoil sample consisting of five 145 cm³ soil cores (0–7.5 cm depth) was collected from each quadrat, bulked, and homogenized in the field (five composite samples per plot were obtained). After field collection, the soil samples were taken to the laboratory, where they were sieved (2 mm mesh). Once sieved, samples were air-dried for one month and stored for physico-chemical analyses. Dried soil samples from all the countries were shipped to the laboratory of Rey Juan Carlos University in Móstoles (Spain) for analyses. Once in the laboratory, replicated soil samples were bulked to obtain a composite sample per plot. Total C and N concentration in soils was determined on ball-milled soils by dry combustion, gas chromatography and thermal conductivity detection, after removing carbonates by acid fumigation. Total P, K, Mg, Ca, Cu, Zn, S, Na, Fe, Al, Mn and Ba were extracted by open-vessel nitric-perchloric acid wet digestion, re-suspended in water, and measured by inductively coupled plasma optical emission spectrometry^{67,68} (ICP-OES Perkin Elmer Optima 4300 DV).

Soil pH was measured in all the soil samples with a pH meter, in a 1:1 soil to water (w:v) suspension⁵². Soil texture (sand, clay and silt content) was measured according to ref. 69. The three textural variables measured (sand, clay and silt) were highly intercorrelated (Spearman $\rho_{\text{sand-silt}} = -0.987, P < 0.001$; Spearman $\rho_{\text{sand-clay}} = -0.851, P < 0.001$; Spearman $\rho_{\text{silt-clay}} = 0.766, P < 0.001$). Thus, we selected just one of these fractions (sand), to use in our data analyses because this fraction is less prone to measurement errors given the method used.

Data management and gap-filling procedure

We compiled a database of 133,769 trait measurements, where each species in each plot was tagged as a unique ID (Supplementary Table 3). Species taxonomy was standardized according to World of Flora (World Flora Online (2023); <http://www.worldfloraonline.org>). 99.5% of the individual plants were identified at the genus level, and 93.6% at the species level. We used pseudo-species names for the 6.4% of species ($n = 18$ species) that could not be identified. To ensure a high level of data quality, all trait measurements were inspected using a semi-automated procedure and corrected when possible following guidelines from ref. 11. Specifically, we looked for potential systematic errors, including wrong units or the presence of aberrant traits values for each species and trait measured.

Morphological traits (H , LS , LL , LA , SLA and $LDMC$) were available at the individual level (20,961 individual plants measured). Traits related to leaf nutrients were available at the plot level for each species. To homogenize the level of analysis for all traits, we averaged individual morphological measurements to obtain a single trait value for each species in each of the 326 plots. For H and LS , we also recorded the maximum value observed in each plot and for each species to characterize plant species maximum H and LS following ref. 57.

Data completeness varied among traits (Supplementary Table 3) but overall offered a high degree of representativeness and geographical coverage at a global scale (Fig. 1). We did not have missing data for morphological traits (H , LS , LL). The levels of data completeness for LA , SLA , $LDMC$ were very high: 95%, 93%, and 89%, respectively. Missing data for these variables were mainly due to methodological reasons, such as the inability to ensure a proper leaf rehydration when measuring leaf fresh mass for $LDMC$. The amount of leaf dry material sampled in the field was lower than the minimum required for some analyses for rare species (for which the leaves of less than three individuals per plot were sampled). Thus, the number of trait samples also differed among leaf nutrients (C/N versus other macro- and microelements) due to the amount of leaf dry material available for analyses (2 mg of dry mass for C/N analyses versus 800 mg of dry mass for other elements). In total, the level of data completeness for chemical traits was greater than 70% for C and N concentration in leaves and greater than 50% for other macro and microelements (Supplementary Table 3).

Data completeness is a fundamental prerequisite of trait covariation analyses because multivariate analyses require a full set of trait information for all species considered. Indeed, a missing value for one trait leads to systematic deletion of the whole species. Therefore, a gap-filling procedure in the data trait matrices is a suitable approach to reduce this problem^{70–72}. Here, we used a highly conservative gap-filling procedure based on the following criteria: (1) we used only trait data measured from our trait sampling (that is, we did not retrieve trait data from external databases such as TRY¹¹); (2) the gap-filling procedure was performed within species in all cases (that is, only when trait values were available for the same species in another plot); and (3) we developed an algorithm to optimize the gap-filling procedure according to both aridity and grazing pressure levels instead of using phylogenetic relatedness⁷³. Specifically, when a trait value is missing for a given species in a given plot, the algorithm allows filling the missing data by maximizing the match between the species trait value and the local environmental conditions (see all details of the gap-filling procedure in Supplementary Text 3 and Supplementary Figs. 13–15). Gap filling significantly improved data representativeness by increasing the number of species considered (Supplementary Table 3) without biasing the trait database. Indeed, we observed remarkably low imputation errors ($11 \pm 8\%$) for most chemical traits, indicating that within species trait variability of the plant elementome is negligible compared to what is observed across species (see additional results in Supplementary Text 3 and Supplementary Figs. 7 and 8).

At the end of the procedure, a total of 1,347 observations of 301 dryland plant species measured across the 326 plots with the complete set of traits were available for analyses (compared to 887 observations before gap filling, see Supplementary Table 3 and Supplementary Fig. 16). The $n = 1,347$ observations were consistently used in all main analyses.

Statistics and reproducibility

We conducted all statistical analyses using the statistical software R 4.3.2 (2023-10-31 ucrt).

Characterizing the dryland trait space. To quantify the trait diversity of dryland plant species, we first determined the fundamental trait dimensions along which dryland plant species segregate. To do this, we ran a series of principal component analyses (PCAs) using the complete set of measured traits (Extended Data Fig. 1) and plant chemical elements only (Supplementary Fig. 5). Traits were log-transformed and scaled before analysis¹² (see the distribution of each trait in Supplementary Figs. 2–4). We used the Horn's parallel analysis from the R package *paran*⁷⁴ to determine the dimensionality of the PCAs¹², and applied a varimax rotation procedure to facilitate the interpretation of the results.

PCAs are standard tools in trait spectrum analyses^{1,12,15,75}. They efficiently summarize the covariations and trade-offs observed among multiple traits by representing the trait loadings (arrows in Extended Data Fig. 1) along the PCA axes (calculated from the eigenvectors of each trait and the eigenvalues of each axis). The percentage of variance explained by each selected axis represents the importance of each PCA dimension in explaining the observed trait variability across species. Eigenvalues were further used to calculate an index of phenotypic integration, which summarizes the strength of trait covariation^{76–78}. This phenotypic integration index was calculated using the variance of the eigenvalues as:

$$\text{Var}(\gamma) = \sum_{i=1}^N (\gamma_i - 1)^2 / N \quad (1)$$

where γ_i is the eigenvalue from the i th dimension and N is the number of traits⁷⁹. We used the eigenvalue of the un-rotated PCA to compute the phenotypic integration index. Higher values of this index indicate stronger covariations among N traits. When traits are uncorrelated, eigenvalues are similar and exhibit low variance. When traits are highly correlated, the first eigenvalue is much higher than the other eigenvalues, leading to high variance. PCA axes also provide information on the hypervolume^{1,38,80,81} occupied by the studied species in a n -dimensional trait space, and thus the size of the hypervolume provides a measure of the trait diversity observed for a given species pool⁸⁰. In this study, we used both hypervolumes and trait covariations to quantify the effects of aridity and grazing on the spectrum of plant traits observed in global drylands.

Evaluating the impacts of aridity on the dryland plant trait space.

We used a sliding-window analysis to evaluate how the hypervolume and trait covariation changed along the aridity gradient evaluated. This analysis is well suited to investigate how the correlation between different variables (here traits) change according to a third predictor (here aridity), and to evaluate whether these changes are linear or abrupt^{48,82,83}. To do so, we first ordered the 326 plots surveyed according to their aridity level. We then selected all plots located within an aridity window of 0.1 (roughly equivalent to 19% of the total aridity gradient captured in our survey), starting from the lowest aridity value observed in our dataset. The width of the aridity window used was selected to ensure: (1) enough statistical power (307 observations of dryland plant species on average within each window; with minimum = 103 and maximum = 473); (2) that the species pools selected in each window originated from plots characterized by different

grazing pressure levels; and (3) that the selected species belonged to contrasted biogeographical regions across the world. Indeed, each aridity window included on average 19 sites (minimum = 8; maximum = 32) originated from different regions of the world to avoid spatial autocorrelation (see Fig. 1). Therefore, our sliding-windows analysis operates at a global scale to evaluate how global increases in aridity and grazing pressure influence the trait pool in drylands worldwide.

For each aridity window, we calculated the strength of trait covariations using the same PCA procedure as explained above and the diversity of trait values observed within this aridity range. We randomly sampled $n = 100$ observations within the window and extracted the eigenvalue of the significant selected axes, calculating their variance to obtain an index of phenotypic integration. We repeated the random sampling of $n = 100$ observations for 100 times within each window to calculate the confidence interval of the index for each aridity window. We used the same procedure to calculate the hypervolume using the R package Hypervolume⁸¹. To calculate the hypervolume, we used the PCA coordinates as trait values for the five dimensions of the dryland plant spectrum described in Extended Data Fig. 4. We then moved the sliding window toward higher aridity levels of 0.01 by both adding the plots scoring the next aridity value and removing the plots with the lowest aridity. We repeated this analysis as many times as plots remained along the aridity gradient. We then plotted the results and tested how trait covariations in the dryland species pool and their diversity changed along the aridity gradient.

We evaluated whether the observed trait responses along the aridity gradient truly corresponded to an aridity-threshold by fitting threshold models using the R package chngpt⁸⁴. In essence, these models find a breakpoint in the data by dividing it according to a predictor value (here aridity) and using two different fitting functions at each side of the breakpoint. To assess whether these threshold models were a better fit to the data than a linear model we used the Bayesian information criterion (BIC), which measures the goodness of fit of the data based on log-likelihood of the fitting functions considering the number of parameters used⁸². The models exhibiting the lowest BIC values are the most parsimonious and provide the best fit. Differences in BIC < 2 represent similarly good models⁸⁵. Apart from a regular linear model, we used a generalized additive model and five different threshold models for extracting the BIC, each differing from each other by the functions fitted at both sides of the estimated breakpoint: step (two intercept models, for which the differences in intercept were tested at the breakpoint), segmented (two linear models in which the slope is changed at breakpoint), stegmented (two linear models in which both the slope and the intercept are changed at the breakpoint), hinge model 12 (one linear model is fitted for the left part of the breakpoint and a second degree polynomial is fitted for the right part), and hinge model 22 (two different second degree polynomial models are fitted at both sides of the breakpoint). The model (either linear or threshold-like) exhibiting the lowest BIC was considered the best model. Each of the threshold models considered allows the identification of a breakpoint with associated 95% confidence interval as a parameter resulting from the model fitting. We considered the aridity value at which a breakpoint was observed as the aridity threshold.

We observed non-linear, abrupt responses of trait covariations and hypervolumes at aridity -0.7 based on the breakpoint analyses described above (Figs. 2 and 3). To further examine how aridity reshaped the dryland plant trait spectrum, we divided our data into two subsets: below and above aridity = $0.7 \pm$ confidence interval. We re-ran all the PCA analyses explained above to evaluate how aridity changed the dimensionality of the trait spectrum for these subsets of the data. We also re-calculated the hypervolume observed at low and high aridity values, and quantified their overlap using the function hypervolume_overlap_statistics in the R package Hypervolume⁸¹. This function provides the percentage of overlap between distinct hypervolumes, as well as the percentage of uniqueness of each hypervolume.

Assessing the impacts of grazing on the dryland plant trait space.

To test for the effects of grazing pressure, we calculated the index of trait covariation and the hypervolumes for each grazing pressure level (ungrazed, low, medium, and high grazing pressure). We used a bootstrap procedure and repeated the calculation 100 times to obtain the confidence interval. We then tested whether different grazing pressure levels showed contrasted values of these indices using a generalized least squares model to account for heteroscedasticity (using the functions from the R package nlme⁸⁶). To represent how different grazing pressures may alter the dryland plant trait space, we also re-ran the PCA analyses for each grazing pressure level evaluated (from ungrazed to high grazing pressure). Finally, we tested whether grazing pressure changed the shape and the location of the aridity threshold. To do so, we re-ran the sliding-windows analysis conducted above, but at each grazing level separately. We tested whether grazing pressure (ungrazed, low, medium and high grazing pressure) changed the location of the threshold. We extracted the bootstrap distribution of the threshold at each grazing pressure level, and tested, using generalized least square models, whether the location of the threshold was significantly shifted along the aridity gradient compared to the overall threshold found at aridity -0.7 .

Assessing the impacts of aridity and grazing on the soil elementome.

We examined how chemical elements in soils (the soil elementome) responded to changes in aridity. We first conducted a PCA as explained above to evaluate how the concentrations of the 14 chemical elements in soils covary across the 326 sampled plots. We then extracted the principal component coordinate of each selected axis and evaluated how the soil elementome responded to grazing and aridity using linear mixed effect models and the R package lme4⁸⁷. We considered in the model the effect of grazing and aridity and used site as a random factor (random effect: 1|site), allowing model intercept to vary among sites since plots belonging to the same site correspond to a local grazing gradient that has been repeated across the 98 sites surveyed. Finally, we used the same sliding-windows procedure as explained above to test how soil chemical diversity responded to aridity. All soil elements covaried along a unique principal component axis accounting for 65.8% of the total variation (Extended Data Fig. 5a,b). Because computing hypervolumes in one dimension is irrelevant⁸¹, we therefore computed the sliding-window analysis only to test whether covariation among multiple soil elements changed with increasing aridity (Extended Data Fig. 5c).

Plant cover as a modulator of the effects of aridity and grazing on the dryland plant trait space.

We evaluated how changes in plant cover observed across global drylands once the -0.7 aridity threshold is crossed impacted on plant trait diversity. We first tested how aridity and grazing impacted plant cover using linear mixed effect models and the R package lme4⁸⁷. Our model included aridity, grazing, and an interaction between them. Site was used as a random factor (random effect: 1|site). The model also included a series of covariates known to impact plant cover⁶ in drylands, such as latitude and longitude of our study sites, as well as their elevation and topography (slope and aspect). We used the sine and cosine of the longitude and aspect to avoid any bias due to intrinsic circularity of these predictors in the statistical models²² (that is, longitude (sin) and longitude (cos) hereafter, respectively). We also considered two soil master variables (sand content and soil pH^{22,88}). A quadratic term was considered for pH. All predictors were scaled before analysis to facilitate the comparison of estimates.

The full model used was: lmer (Plant Cover ~ (1|site) + latitude + longitude (sin) + longitude (cos) + exposure (sin) + exposure (cos) + slope + elevation + aridity \times grazing + sand + pH + pH²). Using this full model, we ran a model averaging procedure to select the set of predictors that best explained variations in plant cover. To do this, we applied a multi-model inference procedure using the MuMIn

Article

R package⁸⁹. This method allowed us to create a set of models with all possible combinations of the initial variables, which were fitted using a maximum likelihood procedure⁹⁰ and sorted according to the Akaike information criterion. Aridity and grazing were the main drivers of plant cover in our analyses (Extended Data Fig. 6). Finally, we substituted aridity by plant cover in our sliding-windows procedure to test how plant cover influenced hypervolume and trait covariation (Extended Data Fig. 7).

Reporting summary

Further information on research design is available in the Nature Portfolio Reporting Summary linked to this article.

Data availability

All processed datasets generated during the current study are available in the open source repository at <https://doi.org/10.57745/SFCXOO>.

Code availability

The R code used to analyse the data is available in the open source repository at <https://doi.org/10.57745/SFCXOO>.

- ILRI et al. *Rangelands Atlas* (ILRI, 2021).
- Maestre, F. T. et al. The BIODESERT survey: assessing the impacts of grazing on the structure and functioning of global drylands. *Web Ecol.* **22**, 75–96 (2022).
- Poppenwimer, T., Mayrose, I. & DeMalach, N. Revising the global biogeography of annual and perennial plants. *Nature* **624**, 109–114 (2023).
- García-Palacios, P., Gross, N., Gaitán, J. & Maestre, F. T. Climate mediates the biodiversity–ecosystem stability relationship globally. *Proc. Natl Acad. Sci. USA* **115**, 8400–8405 (2018).
- Maestre, F. T. et al. Plant species richness and ecosystem multifunctionality in global drylands. *Science* **335**, 214–218 (2012).
- Le Bagousse-Pinguet, Y. et al. Phylogenetic, functional, and taxonomic richness have both positive and negative effects on ecosystem multifunctionality. *Proc. Natl Acad. Sci. USA* **116**, 8419–8424 (2019).
- Cornelissen, J. H. C. et al. A handbook of protocols for standardised and easy measurement of plant functional traits worldwide. *Aust. J. Bot.* **51**, 335–380 (2003).
- Pérez-Harguindeguy, N. et al. Corrigendum to: New handbook for standardised measurement of plant functional traits worldwide. *Aust. J. Bot.* **64**, 715–716 (2016).
- Wright, I. J. et al. Global climatic drivers of leaf size. *Science* **357**, 917–921 (2017).
- Deraison, H., Badenhausser, I., Börger, L. & Gross, N. Herbivore effect traits and their impact on plant community biomass: an experimental test using grasshoppers. *Funct. Ecol.* **29**, 650–661 (2015).
- Cruz, P. et al. Leaf traits as functional descriptors of the intensity of continuous grazing in native grasslands in the south of Brazil. *Rangeland Ecol. Manag.* **63**, 350–358 (2010).
- Salt, D. E., Baxter, I. & Lahner, B. Ionomics and the study of the plant ionome. *Annu. Rev. Plant Biol.* **59**, 709–733 (2008).
- Gaucherand, S. & Lavorel, S. New method for rapid assessment of the functional composition of herbaceous plant communities. *Austral Ecology* **32**, 927–936 (2007).
- Gross, N., Börger, L., Duncan, R. P. & Hulme, P. E. Functional differences between alien and native species: do biotic interactions determine the functional structure of highly invaded grasslands? *Funct. Ecol.* **27**, 1262–1272 (2013).
- Siefert, A. et al. A global meta-analysis of the relative extent of intraspecific trait variation in plant communities. *Ecol. Lett.* **18**, 1406–1419 (2015).
- Schneider, C. A., Rasband, W. S. & Eliceiri, K. W. NIH Image to ImageJ: 25 years of image analysis. *Nat. Methods* **9**, 671–675 (2012).
- Varley, J. A. *A Textbook of Soil Chemical Analysis* by P. R. Hesse London: John Murray (1971), pp. 520, £7.50. *Exp. Agric.* **8**, 184 (1972).
- Kuo, S. in *Methods of Soil Analysis: Part 3 Chemical Methods* (eds Sparks, D. L. et al.) 869–919 (John Wiley & Sons, 1996); <https://doi.org/10.2136/sssabookser5.3.c32>.
- Kettler, T. A., Doran, J. W. & Gilbert, T. L. Simplified method for soil particle-size determination to accompany soil-quality analyses. *Soil Sci. Soc. Am. J.* **65**, 849–852 (2001).
- Penone, C. et al. Imputation of missing data in life-history trait datasets: which approach performs the best? *Methods Ecol. Evol.* **5**, 961–970 (2014).
- Poyatos, R., Sus, O., Badiella, L., Mencuccini, M. & Martínez-Vilalta, J. Gap-filling a spatially explicit plant trait database: comparing imputation methods and different levels of environmental information. *Biogeosciences* **15**, 2601–2617 (2018).
- Jetz, W. et al. Monitoring plant functional diversity from space. *Nat. Plants* **2**, 16024 (2016).
- Swenson, N. G. Phylogenetic imputation of plant functional trait databases. *Ecography* **37**, 105–110 (2014).
- Dinno, A. PARAN: Stata module to compute Horn's test of principal components/factors. *IDEAS* <https://ideas.repec.org/c/boc/bocode/s420702.html> (2009).
- Bueno, C. G. et al. Reply to: The importance of trait selection in ecology. *Nature* **618**, E31–E34 (2023).
- Laughlin, D. C. et al. Intraspecific trait variation can weaken interspecific trait correlations when assessing the whole-plant economic spectrum. *Ecol. Evol.* **7**, 8936–8949 (2017).

- Brown, A., Butler, D. W., Radford-Smith, J. & Dwyer, J. M. Changes in trait covariance along an orographic moisture gradient reveal the relative importance of light- and moisture-driven trade-offs in subtropical rainforest communities. *New Phytol.* **236**, 839–851 (2022).
- Delhaye, G. et al. Interspecific trait integration increases with environmental harshness: a case study along a metal toxicity gradient. *Funct. Ecol.* **34**, 1428–1437 (2020).
- Cheverud, J. M., Wagner, G. P. & Dow, M. M. Methods for the comparative analysis of variation patterns. *Syst. Biol.* **38**, 201–213 (1989).
- Blonder, B. Hypervolume concepts in niche- and trait-based ecology. *Ecography* **41**, 1441–1455 (2018).
- Blonder, B. et al. New approaches for delineating *n*-dimensional hypervolumes. *Methods Ecol. Evol.* **9**, 305–319 (2018).
- Berdugo, M., Gaitán, J. J., Delgado-Baquerizo, M., Crowther, T. W. & Dakos, V. Prevalence and drivers of abrupt vegetation shifts in global drylands. *Proc. Natl Acad. Sci. USA* **119**, e2123393119 (2022).
- Berdugo, M., Kéfi, S., Soliveres, S. & Maestre, F. T. Plant spatial patterns identify alternative ecosystem multifunctionality states in global drylands. *Nature Ecol. Evol.* **1**, 0003 (2017).
- Fong, Y., Huang, Y., Gilbert, P. B. & Permar, S. R. chngpt: threshold regression model estimation and inference. *BMC Bioinformatics* **18**, 454 (2017).
- Schwarz, G. Estimating the dimension of a model. *Ann. Stat.* **6**, 461–464 (1978).
- Pinheiro, J. et al. nlme: Linear and nonlinear mixed effects models. R package version 3 <https://doi.org/10.32614/CRAN.package.nlme> (2017).
- Bates, D. et al. lme4: Linear mixed-effects models using Eigen and S4. R package version 1.1-35.1 <https://doi.org/10.32614/CRAN.package.lme4> (2024).
- Maire, V. et al. Global effects of soil and climate on leaf photosynthetic traits and rates. *Global Ecol. Biogeogr.* **24**, 706–717 (2015).
- Bartoň K. MuMIn: Multi-model inference. R package version 1.48.4, <https://CRAN.R-project.org/package=MuMIn> (2024).
- Zuur, A. F., Ieno, E. N., Walker, N., Saveliev, A. A. & Smith, G. M. *Mixed Effects Models and Extensions in Ecology with R* (Springer, 2009).

Acknowledgements We acknowledge S. Undrakhbold, M. Uuganbayar, B. Byambatsogt, S. Khaliun, S. Solongo, B. Batchuluun, M. Sloan, S. Spann, J. Spence, E. Geiger, I. Souza, R. Onoo, T. Araújo, M. Mabaso, P. M. Lunga, L. Eloff, J. Sebei, J. J. Jordaan, E. Mudongo, V. Mokoka, B. Mokhou, T. Maphanga, D. Thompson, A. S. K. Frank, R. Matjea, F. Hoffmann, C. Goebel, B. Semple, B. Tamayo, R. Peters, A. L. Piña, R. Ledezma, E. Vidal, F. Perona, J. M. Alcántara, A. Howell, R. Reibold, N. Melone, M. Starbuck, E. Geiger, Bush Heritage Australia, the University of Limpopo, Comunidad Agrícola Quebrada de Talca, Conaf Chile and South African Environmental Observation Network (SAEON) for assistance with field work and plant identification, the South African Military for assistance with field work and/or granting access to their properties, and the Scientific Services Kruger National Park. This research was funded by the European Research Council (ERC Grant agreement 647038 1004 [BIODESERT]) and Generalitat Valenciana (CIDEGENT/2018/041). N.G. was supported by CAP 20–25 (16-IDEX-0001) and the AgreenSkills+ fellowship programme which has received funding from the European Union's Seventh Framework Programme under grant agreement FP7-609398 (AgreenSkills+ contract). F.T.M. acknowledges support from the King Abdullah University of Science and Technology (KAUST), the KAUST Climate and Livability Initiative, the University of Alicante (UADIF22-74 and VIGROB22-350), the Spanish Ministry of Science and Innovation (PID2020-116578RB-I00), and the Synthesis Center (sDiv) of the German Centre for Integrative Biodiversity Research Halle–Jena–Leipzig (iDiv). Y.L.B.-P. was supported by Marie Skłodowska-Curie Actions Individual Fellowship (MSCA-1018 IF) within the European Program Horizon 2020 (DRYFUN Project 656035). H.S. is supported by a María Zambrano fellowship funded by the Ministry of Universities and European Union-Next Generation plan. L.W. acknowledges support from the US National Science Foundation (EAR 1554894). G.M.W. acknowledges support from the Australian Research Council (DP210102593) and TERN. M.B. is supported by a Ramón y Cajal grant from Spanish Ministry of Science (RYC2021-031797-I). L.v.d.B. and K.T. were supported by the German Research Foundation (DFG) Priority Program SPP-1803 (TI388/14-1). A.F. acknowledges the financial support from ANID PIA/BASAL FB210006 and Millenium Science Initiative Program NCN2021-050. A.J. was supported by the Bavarian Research Alliance for travel and field work (BayIntAn UBT 2017 61). A.L. and L.K. acknowledge support from the German Research Foundation, DFG (grant CRC TRR228) and German Federal Government for Science and Education, BMBF (grants O1LL1802C and O1LC1821A). B.B. and S.U. were supported by the Taylor Family-Asia Foundation Endowed Chair in Ecology and Conservation Biology. P.J.R. and A.J.M. acknowledge support from Fondo Europeo de Desarrollo Regional through the FEDER Andalucía operative programme, FEDER-UJA 1261180 project. E.M.-J. and C.P. acknowledge support from the Spanish Ministry of Science and Innovation (PID2020-116578RB-I00). D.J.E. was supported by the Hermon Slade Foundation. J.D. and A. Rodríguez acknowledge support from the FCT (2020.03670. CEECIND and SFRH/BDP/108913/2015, respectively), as well as from the MCTES, FSE, UE and the CFE (UIDB/04004/2021) research unit financed by FCT/MCTES through national funds (PIDDAC). S.C.R. acknowledges support from the US Department of Energy (DE-SC-0008168), US Department of Defense (RC18-1322), and the US Geological Survey Ecosystems Mission Area. Any use of trade, firm, or product names is for descriptive purposes only and does not imply endorsement by the US government. E.H.-S. acknowledges support from Mexican National Science and Technology Council (CONACYT PN 5036 and 319059). A.N. and C. Branquinho. acknowledge the support from FCT—Fundação para a Ciência e a Tecnologia (CEECIND/02453/2018/CP1534/GT0001, PTDC/ASP-SIL/7743/2020, UIDB/00329/2020), from AdaptForGrazing project (PRR-C05-i03-I-000035) and from LTRER Montado platform (LTER_EU_PT_001). Field work of G.P. and J.M.Z. was supported by UNRN (PI 40-C-873).

Author contributions N.G., F.T.M. and Y.L.B.-P. conceived this study. F.T.M., N.G. and Y.L.B.-P. designed and coordinated the global field survey. N.G., P.L. and Y.L.B.-P. developed the original idea of the analyses presented in the manuscript, with inputs from F.T.M., M.B., R.M., M.D.-B., V.M., E.M.-J., H.S., S.S. and E.V. F. Jabot. developed the theoretical model on plant

cover. Fieldwork was done by all co-authors with the assistance of M.G.-G. for field site assessments. Laboratory analyses were done by V.O., B.G., S.A., C.P., M.G.-G. and I.S.P. The trait database was built by N.G., R.M. and Y.L.B.-P. Data and code handling, curation and verification were done by N.G., R.M., V.O., B.G., I.S.P. and Y.L.B.-P. Statistical analyses were performed by N.G., M.B., and R.M. N.G., Y.L.B.-P. and F.T.M. wrote the first manuscript draft and all authors worked on the final version.

Competing interests The authors declare no competing interests.

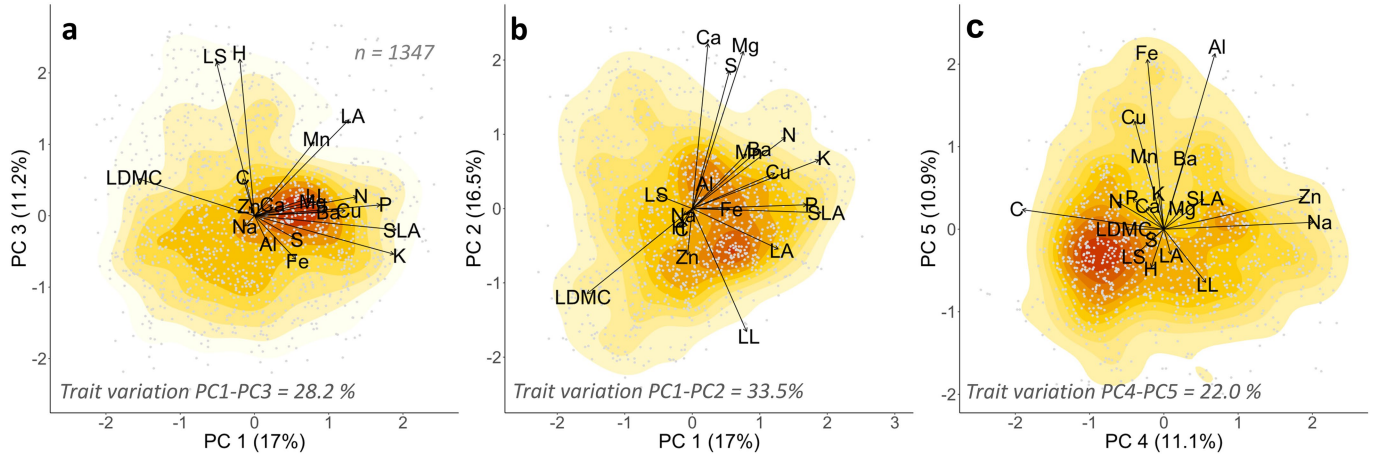
Additional information

Supplementary information The online version contains supplementary material available at <https://doi.org/10.1038/s41586-024-07731-3>.

Correspondence and requests for materials should be addressed to Nicolas Gross, Fernando T. Maestre or Yoann Le Bagousse-Pinguet.

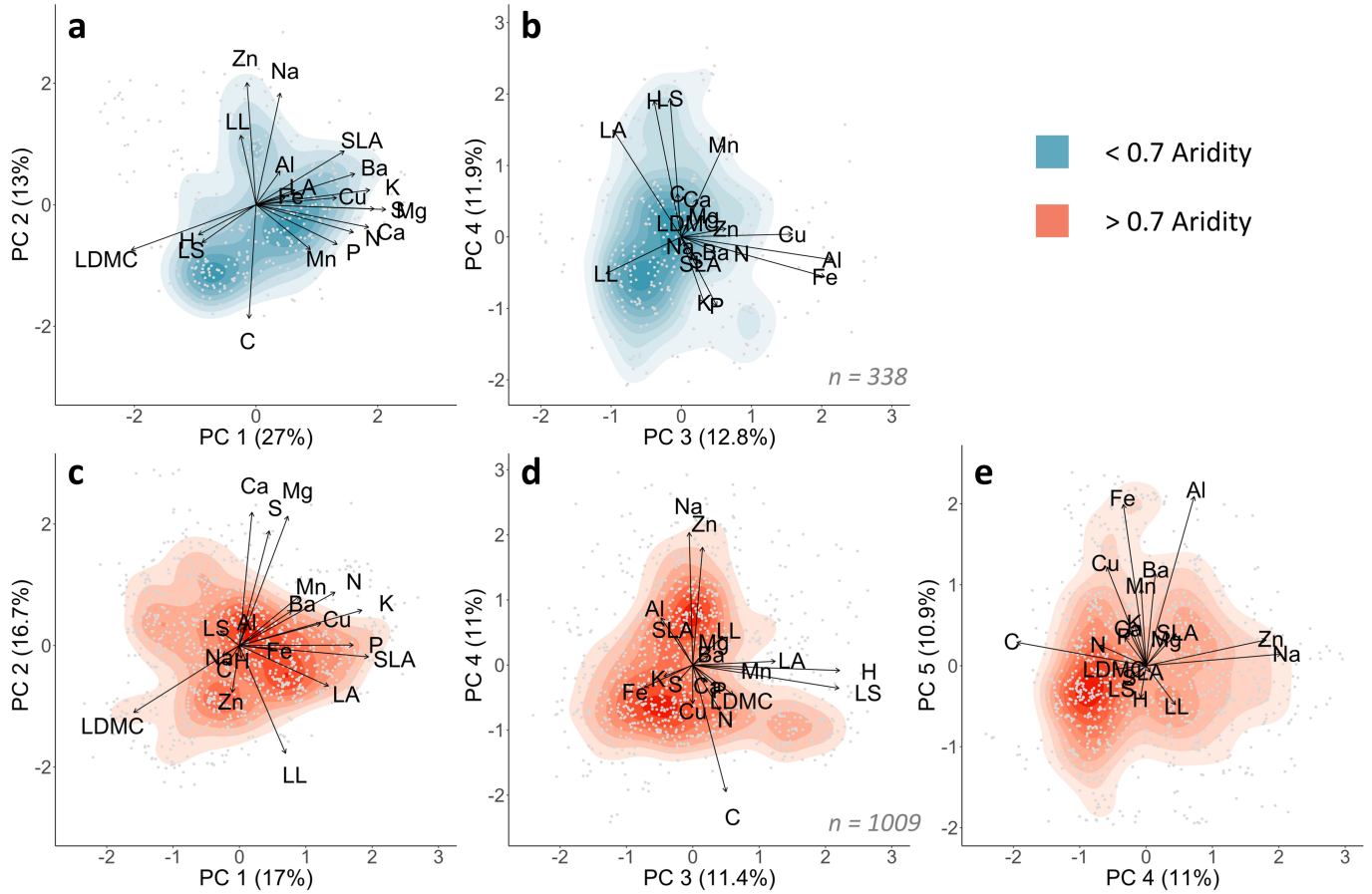
Peer review information *Nature* thanks Stéphane Dray and the other, anonymous, reviewer(s) for their contribution to the peer review of this work. Peer review reports are available.

Reprints and permissions information is available at <http://www.nature.com/reprints>.



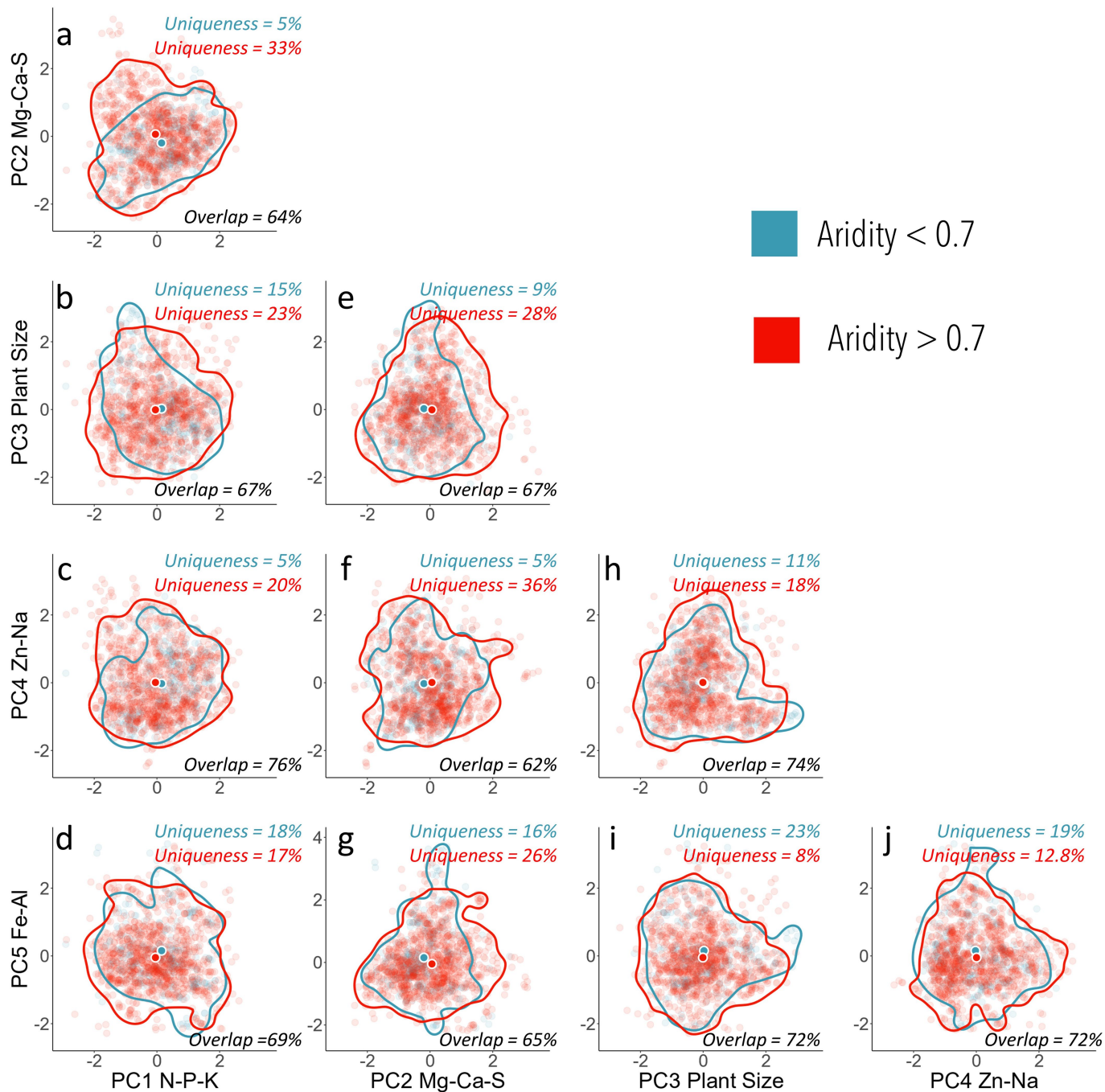
Extended Data Fig. 1 | The trait space of global dryland rangelands. **a-c** represent the probabilistic species distributions in the space defined by a Principal Component Analysis (PCA) on whole-plant and leaf size, and on leaf chemical traits. **a** shows the dimensions related to plant size and leaf C-economy. **b-c** show the additional, but independent dimensions related to the plant elementome characterized by the concentration of 14 elements in plant leaves: C, N, P, Mg, Mn, Ca, Cu, Al, Ba, Fe, K, Na, S, and Zn. The dryland trait space displayed five major dimensions (Principal Components PC1 to PC5), accounting for 66.7% of the total trait variation. In **a**, Leaf traits related to leaf C-economy (PC1) and plant size (PC3) varied along two orthogonal dimensions and accounted for a total of 28.2% of trait variation. In **b-c**, the plant elementome accounted for 55.5% of trait variation. While a dimension of the plant elementome covaried with the leaf C-economy dimension²⁷ (N-P-K on PC1), it also added three other orthogonal dimensions that were associated with important

macro- and micronutrients (PC2, PC4, PC5). These findings show that a large fraction of trait diversity found across global drylands is not captured by plant size and leaf C-economy alone, but by the plant elementome (see Supplementary Fig. 5 for an additional description of the elementome; Supplementary Fig. 8 for the PCA ran without the gap-filling of the data; Supplementary Fig. 7 for pictures of dryland plant species). The color gradient depicts the different species densities in the trait space (high and low density in red and fading yellow, respectively). The arrow length is proportional to the trait loadings. Each point represents the location of a species within the five-dimensional trait space for all the species surveyed ($n = 1347$). Abbreviations: maximum plant height, H; Lateral spread, LS; Leaf length, LL; leaf area, LA; specific leaf area, SLA; leaf dry matter content, LDMC. See also Supplementary Table 4 for detailed results.



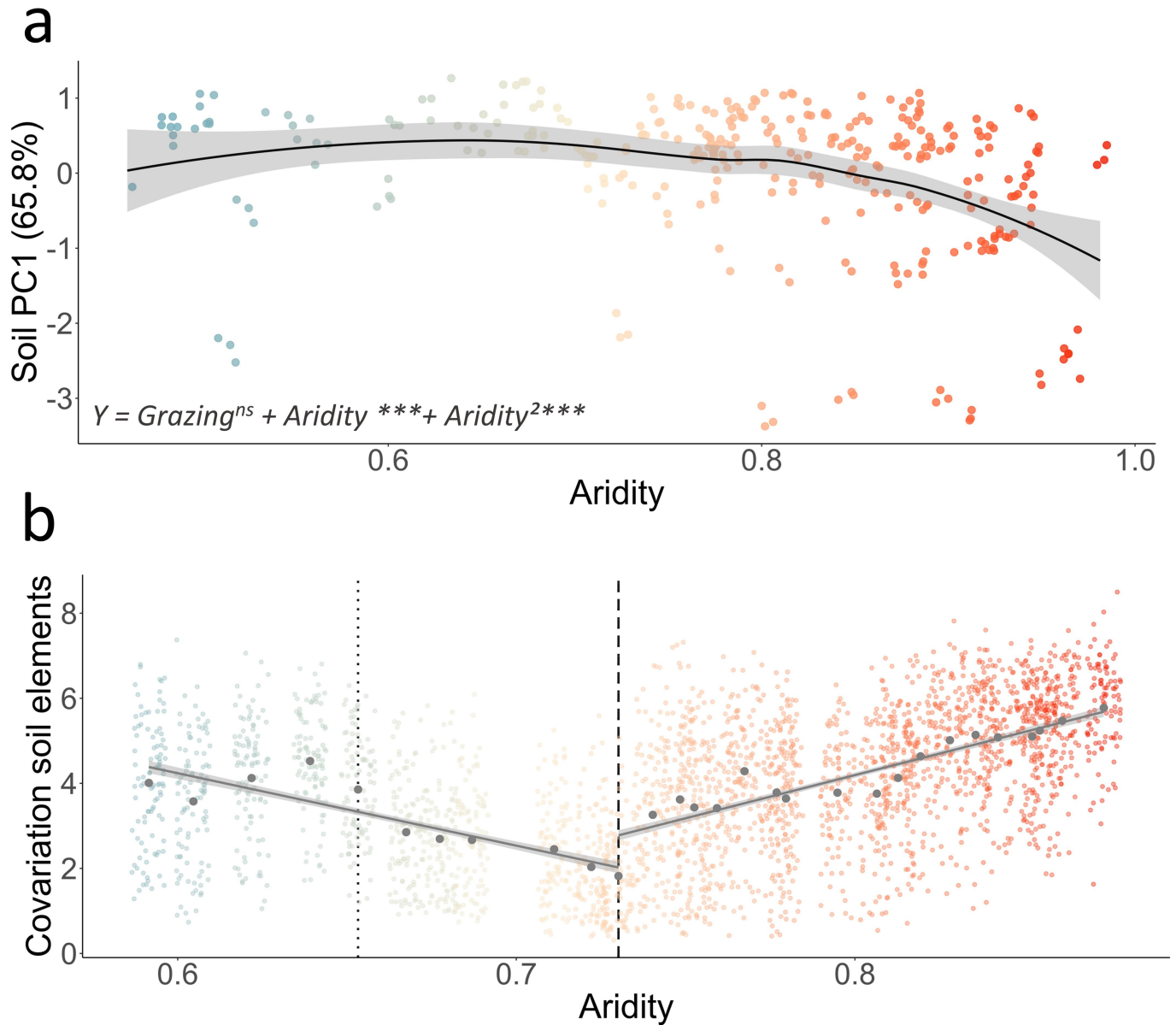
Extended Data Fig. 2 | Aridity reshuffles the trait space of global dryland rangelands. We show how trait covariation changes along the aridity gradient using Principal Component Analysis (PCA) conducted for sites with aridity values located below and above the aridity threshold of -0.7 (Low aridity *n* = 338; high aridity *n* = 1009). The arrow length is proportional to the loadings

of the traits considered. In **a-b**, four principal components were selected at aridity values < 0.7 while in **c-e** five components were selected at aridity values > 0.7. See Extended Data Fig. 1 for trait abbreviations and Supplementary Table 4 for detailed results.



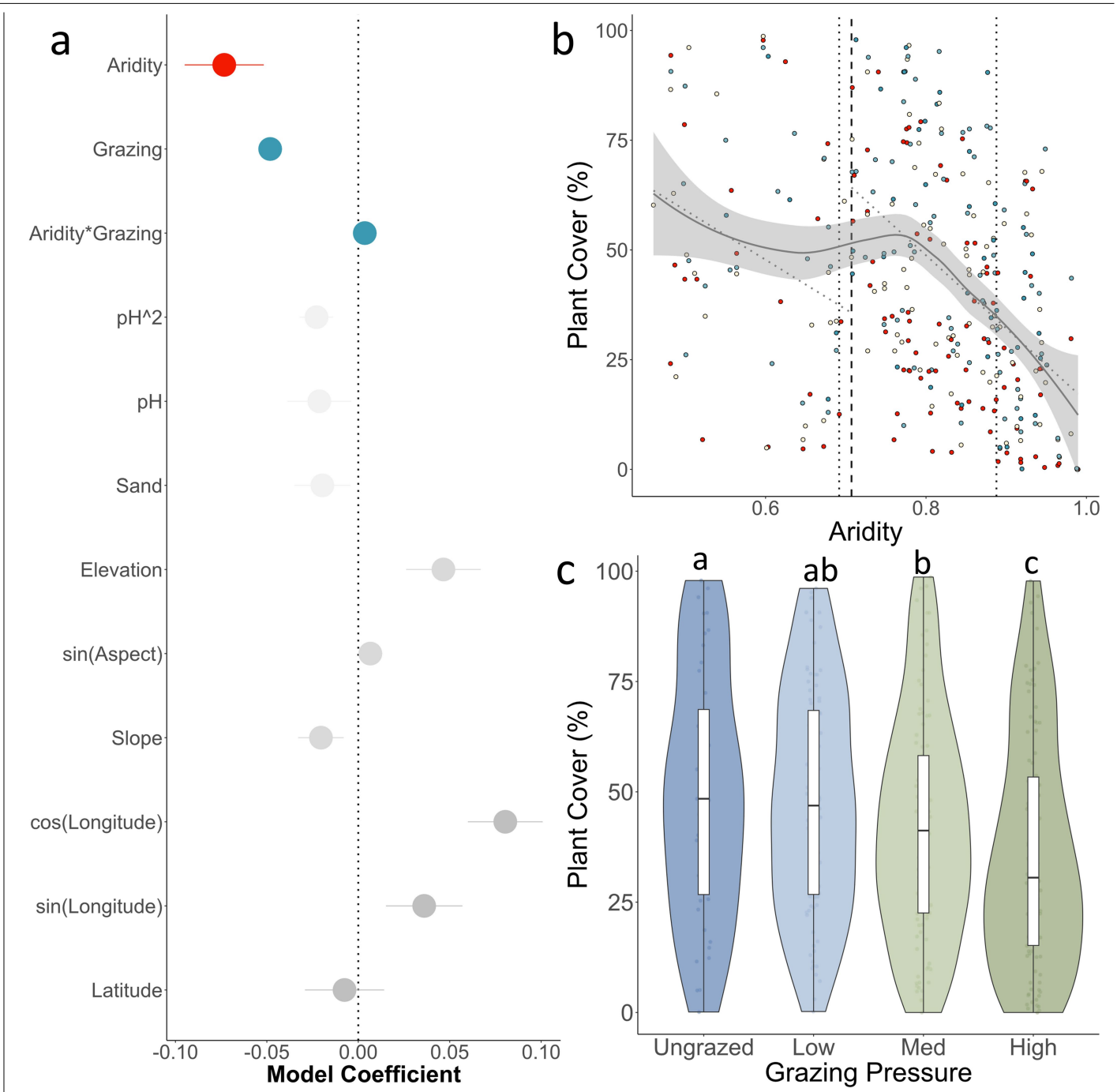
Extended Data Fig. 4 | Representation of the trait hypervolume before and after crossing the -0.7 aridity threshold. We show the 2D projection of the hypervolume for each pair of PCA dimensions shown in Extended Data Fig. 1 (n-dimensions = 5, from PC1 to PC5). Colored dots represent the locations of

each measured species within the trait space. The blue and the red large bright dots represented the centroids of each hypervolume before and after an aridity value of 0.7 (low aridity $n = 189$; high aridity $n = 696$). Colored lines show the 0.95 confidence intervals of the hypervolume before and after this aridity value.



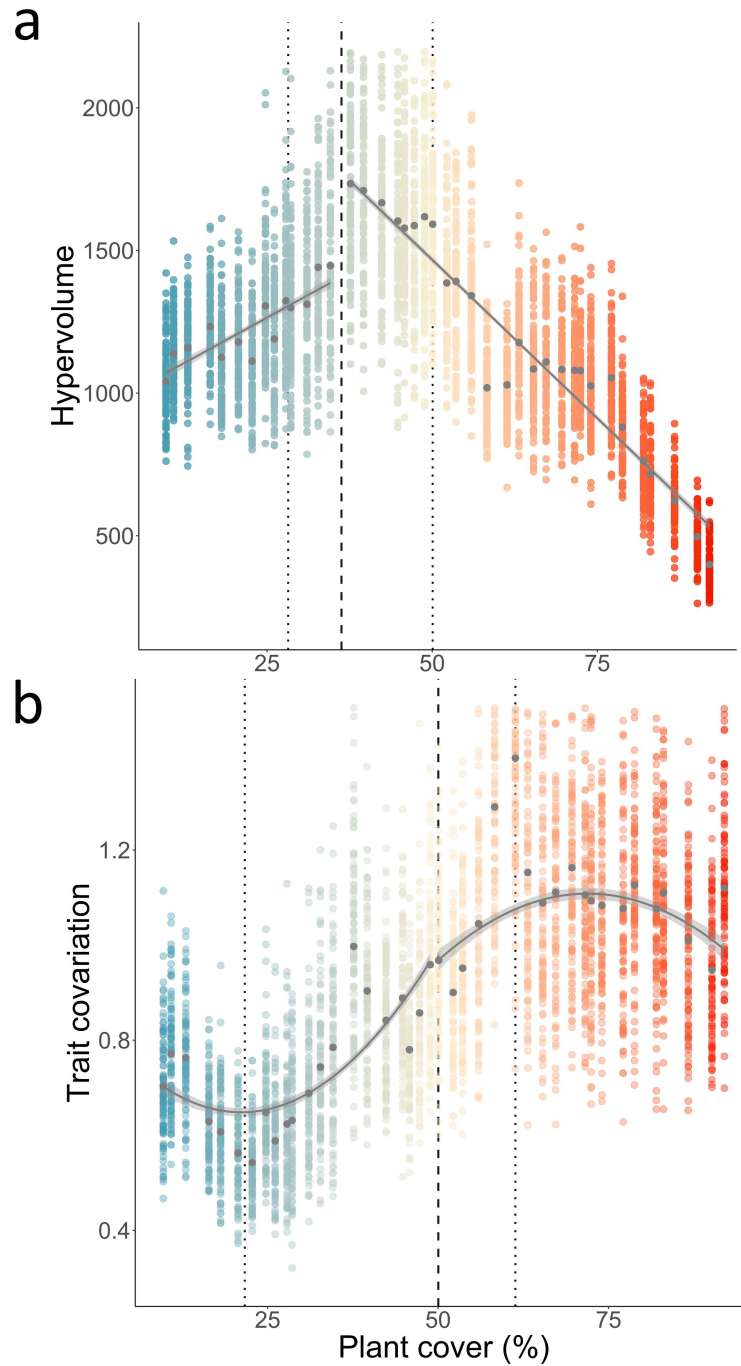
Extended Data Fig. 5 | Response of elemental concentration in soils (the soil elementome) to aridity. Soil elements covary across the 326 sampled plots along a unique Principal Component axis (PC1) that account for 65.8% of soil total variation (see Methods). **a** shows responses of the soil elementome, illustrated using the soil PC 1, to aridity. PC1 shows a quadratic response to aridity with non-linear decrease occurring only in the most arid areas, i.e., those with aridity values > 0.8. Grazing did not modify this response. **b** shows how the soil elementome responded to aridity using a sliding windows analysis (see methods). We first ordered the 326 plots according to their aridity level.

We then defined an aridity window that represented 10% of the global aridity gradient and selected all plots within this aridity range ($n > 30$ plots in each window). We finally examined how the bootstrapped covariation of soil elements across plots changed as aridity increased. We found that aridity further increased the covariation of soil elements in the most arid rangelands surveyed. See Supplementary Table 7 for detailed results of model selections evaluating the response of the soil elementome to aridity. Error band shows the 0.95 confidence interval in **a** and **b**.



Extended Data Fig. 6 | Global decrease in plant cover driven by aridity and grazing. **a** shows the averaged model parameters (± 0.95 confidence interval) for different predictors (i.e. aridity, grazing, soil, and geographical variables) on plant cover ($n = 326$ plots). Significant predictors do not cross the vertical dotted line. Aridity and grazing were the main drivers of plant cover. **b** illustrates the effects of aridity on plant cover. Vertical dashed and dotted lines represent the mean location of the threshold and its 0.95 confidence interval, respectively. Error band shows the 0.95 confidence interval. **c** shows grazing effect on plant cover (High Grazing $n = 98$; Medium Grazing $n = 97$; Low Grazing $n = 88$; Ungrazed $n = 43$). Data are represented as boxplots where the middle line is the

median, the lower and upper hinges correspond to the first and third quartiles, the upper and lower lines show the 0.95 confidence interval. Data beyond the confidence interval are outlying points that are plotted individually. We tested whether different grazing pressure levels showed significant differences using a generalized least squares model ($p < 0.001$). Letters show results of a post-hoc test based on bootstrapped pairwise comparisons between grazing pressure levels. Different letters indicate significant differences among grazing pressure levels. Plant cover decreased non-linearly at aridity -0.7 and was the lowest under high grazing pressure.



Extended Data Fig. 7 | Plant cover mediates the effect of aridity and grazing pressure on trait diversity across global dryland rangelands. a-b show the response of trait diversity (hypervolume and trait covariation respectively) to plant cover using a sliding window procedure (see Methods). Increasing plant cover decreased hypervolume and increased trait covariations, with a

significant threshold value occurring at a plant cover value close to $50\% \pm CI$ (vertical dashed lines, the dotted lines show its 0.95 percentile Confidence Interval, CI). See Supplementary Table 8 for detailed results of model selection evaluating the response of the plant elementome to plant cover. Error band shows the 0.95 confidence interval in **a** and **b**.

Reporting Summary

Nature Portfolio wishes to improve the reproducibility of the work that we publish. This form provides structure for consistency and transparency in reporting. For further information on Nature Portfolio policies, see our [Editorial Policies](#) and the [Editorial Policy Checklist](#).

Statistics

For all statistical analyses, confirm that the following items are present in the figure legend, table legend, main text, or Methods section.

n/a | Confirmed

- The exact sample size (n) for each experimental group/condition, given as a discrete number and unit of measurement
- A statement on whether measurements were taken from distinct samples or whether the same sample was measured repeatedly
- The statistical test(s) used AND whether they are one- or two-sided
Only common tests should be described solely by name; describe more complex techniques in the Methods section.
- A description of all covariates tested
- A description of any assumptions or corrections, such as tests of normality and adjustment for multiple comparisons
- A full description of the statistical parameters including central tendency (e.g. means) or other basic estimates (e.g. regression coefficient) AND variation (e.g. standard deviation) or associated estimates of uncertainty (e.g. confidence intervals)
- For null hypothesis testing, the test statistic (e.g. F , t , r) with confidence intervals, effect sizes, degrees of freedom and P value noted
Give P values as exact values whenever suitable.
- For Bayesian analysis, information on the choice of priors and Markov chain Monte Carlo settings
- For hierarchical and complex designs, identification of the appropriate level for tests and full reporting of outcomes
- Estimates of effect sizes (e.g. Cohen's d , Pearson's r), indicating how they were calculated

Our web collection on [statistics for biologists](#) contains articles on many of the points above.

Software and code

Policy information about [availability of computer code](#)

Data collection

Data analysis

For manuscripts utilizing custom algorithms or software that are central to the research but not yet described in published literature, software must be made available to editors and reviewers. We strongly encourage code deposition in a community repository (e.g. GitHub). See the Nature Portfolio [guidelines for submitting code & software](#) for further information.

Data

Policy information about [availability of data](#)

All manuscripts must include a [data availability statement](#). This statement should provide the following information, where applicable:

- Accession codes, unique identifiers, or web links for publicly available datasets
- A description of any restrictions on data availability
- For clinical datasets or third party data, please ensure that the statement adheres to our [policy](#)

Data availability
All processed datasets generated during the current study are available in the open source repository:
<https://doi.org/10.57745/SFCXOO>

Code availability

The custom R code used to analyze the data is available in the open source repository:

<https://doi.org/10.57745/SFCXOO>

Research involving human participants, their data, or biological material

Policy information about studies with [human participants or human data](#). See also policy information about [sex, gender \(identity/presentation\), and sexual orientation](#) and [race, ethnicity and racism](#).

Reporting on sex and gender

Use the terms sex (biological attribute) and gender (shaped by social and cultural circumstances) carefully in order to avoid confusing both terms. Indicate if findings apply to only one sex or gender; describe whether sex and gender were considered in study design; whether sex and/or gender was determined based on self-reporting or assigned and methods used. Provide in the source data disaggregated sex and gender data, where this information has been collected, and if consent has been obtained for sharing of individual-level data; provide overall numbers in this Reporting Summary. Please state if this information has not been collected. Report sex- and gender-based analyses where performed, justify reasons for lack of sex- and gender-based analysis.

Reporting on race, ethnicity, or other socially relevant groupings

Please specify the socially constructed or socially relevant categorization variable(s) used in your manuscript and explain why they were used. Please note that such variables should not be used as proxies for other socially constructed/relevant variables (for example, race or ethnicity should not be used as a proxy for socioeconomic status). Provide clear definitions of the relevant terms used, how they were provided (by the participants/respondents, the researchers, or third parties), and the method(s) used to classify people into the different categories (e.g. self-report, census or administrative data, social media data, etc.) Please provide details about how you controlled for confounding variables in your analyses.

Population characteristics

Describe the covariate-relevant population characteristics of the human research participants (e.g. age, genotypic information, past and current diagnosis and treatment categories). If you filled out the behavioural & social sciences study design questions and have nothing to add here, write "See above."

Recruitment

Describe how participants were recruited. Outline any potential self-selection bias or other biases that may be present and how these are likely to impact results.

Ethics oversight

Identify the organization(s) that approved the study protocol.

Note that full information on the approval of the study protocol must also be provided in the manuscript.

Field-specific reporting

Please select the one below that is the best fit for your research. If you are not sure, read the appropriate sections before making your selection.

Life sciences Behavioural & social sciences Ecological, evolutionary & environmental sciences

For a reference copy of the document with all sections, see [nature.com/documents/nr-reporting-summary-flat.pdf](https://www.nature.com/documents/nr-reporting-summary-flat.pdf)

Ecological, evolutionary & environmental sciences study design

All studies must disclose on these points even when the disclosure is negative.

Study description

Our study focused on drylands, areas where rainfall is < 65% of the evaporative demand. We surveyed 98 dryland sites located in 25 countries from six continents (Algeria, Argentina, Australia, Botswana, Brazil, Canada, Chile, China, Ecuador, Hungary, Iran, Israel, Kazakhstan, Kenya, Mexico, Mongolia, Namibia, Niger, Palestine, Peru, Portugal, South Africa, Spain, Tunisia, and the United States of America) (see Figure 1 main text). Site selection captured most of the aridity conditions, vegetation (shrublands, grasslands, open woodlands, savannahs, and steppes) and soil types that can be found in drylands worldwide.

Research sample

Vegetation surveys were carried out after the main rainfall season at each site to ensure surveying during (or just after) the main peak biomass. This approach allowed us to standardize the sampling while accounting for differences in vegetation phenology among contrasted biogeographical regions, continents, and hemispheres. We restricted our study to perennial plants because they represent 94% of the plant species on earth and are instrumental in maintaining the functioning of drylands.

Sampling strategy

We focused on 20 continuous traits related to the morphological and chemical diversity of plants, which were measured following the most updated standardized protocols. These traits included: i) whole-plant and leaf size related traits^{1,59} (maximum plant height [H, cm], plant lateral spread [LS, cm²], leaf length [LL, cm] and leaf area [LA, cm²]); ii) leaf traits related to carbon-economy and herbivory^{27,32,40,60,61} (Specific leaf area [SLA, cm².g⁻¹], leaf dry matter content [LDMC, g.g⁻¹]); and iii) the foliar concentration of 14 chemical elements that characterize the plant elementome^{28,29,32,62} (C, N, P, K, Mg, Ca, Zn, S, Na, Cu, Fe, Al, Mn, and Ba).

These traits were measured in situ within each of the 326 plots. To do so, four 45 m transects oriented downslope were established within each plot, and spaced 10 m apart. We then placed 25 contiguous quadrats (1.5 m × 1.5 m) along each transect (100 quadrats per plot). Trait measurements were performed on five quadrats randomly selected in each transect (i.e., five quadrats × four

transects = 20 quadrats per plot). In each quadrat, we selected the most developed individual of each perennial species present.

Our sampling protocol is highly suitable to account for both local trait abundances (because frequent species will have more samples than rare species) and between-plot intraspecific trait variability⁶⁵. See ref.⁵² for a detailed description of the sampling protocol followed.

see more details in the Methods section.

Data collection

Data were collected by all coauthors of the study.

Timing and spatial scale

Fieldwork was conducted between January 2016 and September 2019. Spatial scale global

Data exclusions

We did not exclude data points

Reproducibility

We used standardized protocols in each field location

Randomization

Individual plants were sampled in quadrat that were randomly selected in each sampling location (see methods)

Blinding

Our study is an observational study not a clinical research study. Blinding was not relevant in our case.

Did the study involve field work?

Yes No

Field work, collection and transport

Field conditions

Our study focused on drylands, areas where rainfall is < 65% of the evaporative demand⁵¹. We surveyed 98 dryland sites located in 25 countries from six continents (Algeria, Argentina, Australia, Botswana, Brazil, Canada, Chile, China, Ecuador, Hungary, Iran, Israel, Kazakhstan, Kenya, Mexico, Mongolia, Namibia, Niger, Palestine, Peru, Portugal, South Africa, Spain, Tunisia, and the United States of America). Aridity ranged between 0.48 (wettest) to 0.99 (driest) across the surveyed drylands. This aridity range corresponds to a gradient of mean annual precipitation between 891 and 29 mm/yr, and to a gradient of mean annual temperature between -1.2 and 29.2°C. Our survey also captured most of the variation in grazing pressure that can be found across dryland rangelands worldwide⁶.

Location

(Algeria, Argentina, Australia, Botswana, Brazil, Canada, Chile, China, Ecuador, Hungary, Iran, Israel, Kazakhstan, Kenya, Mexico, Mongolia, Namibia, Niger, Palestine, Peru, Portugal, South Africa, Spain, Tunisia, and the United States of America)

Access & import/export

These shipments were carried out according to national and international regulations; exporting permits were obtained for each country (when required) and importing permits to Spain were obtained for every shipment by the Spanish Ministry of Agriculture, Fisheries and Food.

Disturbance

The sampling did not involve any disturbance

Reporting for specific materials, systems and methods

We require information from authors about some types of materials, experimental systems and methods used in many studies. Here, indicate whether each material, system or method listed is relevant to your study. If you are not sure if a list item applies to your research, read the appropriate section before selecting a response.

Materials & experimental systems

- n/a
- Involvement in the study
- Antibodies
- Eukaryotic cell lines
- Palaeontology and archaeology
- Animals and other organisms
- Clinical data
- Dual use research of concern
- Plants

Methods

- n/a
- Involvement in the study
- ChIP-seq
- Flow cytometry
- MRI-based neuroimaging

Dual use research of concern

Policy information about [dual use research of concern](#)

Hazards

Could the accidental, deliberate or reckless misuse of agents or technologies generated in the work, or the application of information presented in the manuscript, pose a threat to:

- | No | Yes |
|-------------------------------------|---|
| <input checked="" type="checkbox"/> | <input type="checkbox"/> Public health |
| <input checked="" type="checkbox"/> | <input type="checkbox"/> National security |
| <input checked="" type="checkbox"/> | <input type="checkbox"/> Crops and/or livestock |
| <input checked="" type="checkbox"/> | <input type="checkbox"/> Ecosystems |
| <input checked="" type="checkbox"/> | <input type="checkbox"/> Any other significant area |

Experiments of concern

Does the work involve any of these experiments of concern:

- | No | Yes |
|-------------------------------------|--|
| <input checked="" type="checkbox"/> | <input type="checkbox"/> Demonstrate how to render a vaccine ineffective |
| <input checked="" type="checkbox"/> | <input type="checkbox"/> Confer resistance to therapeutically useful antibiotics or antiviral agents |
| <input checked="" type="checkbox"/> | <input type="checkbox"/> Enhance the virulence of a pathogen or render a nonpathogen virulent |
| <input checked="" type="checkbox"/> | <input type="checkbox"/> Increase transmissibility of a pathogen |
| <input checked="" type="checkbox"/> | <input type="checkbox"/> Alter the host range of a pathogen |
| <input checked="" type="checkbox"/> | <input type="checkbox"/> Enable evasion of diagnostic/detection modalities |
| <input checked="" type="checkbox"/> | <input type="checkbox"/> Enable the weaponization of a biological agent or toxin |
| <input checked="" type="checkbox"/> | <input type="checkbox"/> Any other potentially harmful combination of experiments and agents |

Plants

Seed stocks

We samples leaves from plants in the fields. We measured plant height, i.e. the height of the selected individual from the ground to the highest leaves belonging to the vegetative part of the plant; and the lateral spread using two perpendicular measurements of plant width. On the same individual, we then sampled mature and undamaged leaves at the top of the plant to ensure a

Novel plant genotypes

development under full-light conditions (sampled leaf surface was always > 2 cm²).

Authentication

NA